

Neutrino physics

S. Pascoli

Institute for Particle Physics Phenomenology, Department of Physics, Durham University, Durham, United Kingdom

Abstract

The discovery of neutrino oscillations just over 20 years ago has opened a new page in particle physics. It implies that neutrinos have masses and mix and, consequently, that the Standard Model of particle physics is incomplete. The key question we need to answer is: what is the origin of neutrino masses and of leptonic mixing? An impressive effort has been made to paint a precise picture of neutrino mixing. The first hints of CP violation have been reported and hunts for the nature of neutrinos are ongoing. This information guides us in extending the Standard Model to a full theory, advocating new particles and interactions. We will present a concise discussion of these issues, focusing mainly on the theoretical and phenomenological aspects and we will briefly discuss the role of neutrinos in the early Universe and in astrophysical objects.

Keywords

Neutrinos, neutrino oscillations, neutrino masses, leptonic mixing, see-saw mechanism, leptogenesis, lectures.

1 Introduction

Neutrinos are all around us but they remain the most elusive of the known fermionic particles. Their properties might hold the key to unveiling the physics beyond the Standard Model (SM) of particle physics and indeed, together with dark matter, so far they are the only evidence we have that a new theory is required.

We are not far away from the centenary of the idea itself of the neutrino, proposed in December 1930 by W. Pauli. In the 20's physicists were puzzled by the continuous spectrum of β -decays. In this process a nucleus transforms itself into another one with the emission of an electron



Only the parent and daughter nuclei and the electron could be seen. Based on these observations, according to energy-momentum conservation, the electron should carry away an energy corresponding to the difference in mass between parent and daughter nuclei. Therefore there should be a monochromatic line in the β -spectrum, in disagreement with observations. It was Pauli who suggested a possible solution to save the principle of energy-momentum conservation. In a famous open letter sent to the Gauverein meeting in Tübingen, addressed to “Dear Radioactive Ladies and Gentlemen”, Pauli suggests: “I have hit upon a desperate remedy to save... the law of conservation of energy. Namely, the possibility that there could exist in the nuclei electrically neutral particles, that I wish to call neutrons, which have spin 1/2... The continuous beta spectrum would then become understandable by the assumption that in beta decay a neutron is emitted in addition to the electron such that the sum of the energies of the neutron and the electron is constant...” A copy of the letter with English translation is available at [1]. Soon after, J. Chadwick discovered a new heavy neutral particle and named it also the neutron [2]. A new name was needed for Pauli's hypothetical particle, and E. Amaldi playfully called it the “neutrino” in a conversation with E. Fermi, in contrast to his bigger synonymous, the *neutrone*¹. E. Fermi adopted

¹In Italian, the suffix -one indicates something big while -ino is a diminutive.

the name at the Paris Solvay Conference in 1932 and later in 1933. Moreover, Fermi, taking seriously Pauli's idea, constructed the theory of β -decay [3] in 1934, explaining it in terms of a 4-fermion interaction $n \rightarrow pe^{-}\bar{\nu}$ with strength G_F . This interaction would also predict the scattering of neutrinos off matter, via the inverse β process $\bar{\nu}p \rightarrow ne^{+}$. In 1934 Bethe and Peierls were able to estimate the cross section for this process [4], finding it smaller than 10^{-44} cm² for a neutrino energy of 2 MeV. The discouraging implication was that "it was absolutely impossible to observe processes of this kind". It was B. Pontecorvo who suggested that indeed one could use the large neutrino fluxes becoming available [5] due to the advances in nuclear energy at the time. After unfruitfully considering the use of a nuclear explosion, F. Reines and C. L. Cowan devised a method to detect antineutrinos coming from a nuclear reactor. This technique, still in use today, exploits the simultaneous emission of a neutron and a positron in inverse beta decays to significantly reduce backgrounds. Indeed, in 1956 at the Savannah River Plant in South Carolina, they were able to detect neutrinos [6] and soon wrote a telegram to Pauli to inform him that they had "definitely detected neutrinos from fission fragments". Reines received the Nobel Prize in Physics for this discovery in 1995.

Although it was assumed for a long time that parity was an obvious symmetry of nature, in the 50's the idea that it is not conserved in weak interactions started to emerge, mainly thanks to the work of T. D. Lee and C. N. Yang [7]. Soon after, in 1956, Madame Wu and collaborators were able to prove that parity is violated in the β -decay of polarised ⁶⁰Co [8] and in 1958 M. Goldhaber, L. Grodzins and A. W. Sunyar [9] showed that neutrinos are polarised in the opposite direction to their motion, i.e. they are left-handed. Landau [10], Lee and Yang [11] and Salam [12] proposed that neutrinos can be described with a left-handed Weyl spinor. This property was embedded in the $V - A$ theory of weak interactions and ultimately in the Standard Model (SM) of particle physics by S. L. Glashow [13], S. Weinberg [14] and A. Salam [15], spectacularly confirmed by the discovery of the W and Z bosons in 1983 and of the Higgs boson in 2012.

The idea that neutrinos and antineutrinos could be indistinguishable was due to Majorana in 1937 [16]. This question turns out to be intrinsically linked to the conservation or not of lepton number. The latter symmetry was first introduced by E. J. Konopinski and H. M. Mahmoud in 1953 to explain some missing decay modes [17]. Leptons, i.e. the electron, muon and tau and the neutrinos are given lepton number 1 and their antiparticles lepton number -1 . The Reines and Cowan experiment preserves lepton number while searches for solar electron antineutrinos, carried out by R. Davis soon after, did not lead to any positive result. Indeed they break lepton number by two units. Davis will go on to detect electron neutrinos from the sun with the Homestake experiment.

Another important chapter in the understanding of neutrinos concerns the concept of families or generations. The muon was discovered in 1937 by J. C. Street and E. C. Stevenson [18] and by S. H. Neddermeyer and C. D. Anderson [19]. Being a heavier version of the electron, it enters Fermi interactions accompanied by a neutrino. The question was if this neutrino was the same as the one in beta decays or a different type. Following a suggestion by Pontecorvo [20], in 1962 L. M. Lederman, M. Schwartz and J. Steinberger *et al.* created the first accelerator neutrino beam, from pion decays from a boosted proton beam hitting a target, and showed that the neutrinos produced in pion decays associated with a muon do not lead to electrons in scatterings off matter [21]. Indeed, this is the proof that there are two types of neutrinos, electron and muon neutrinos and that they participate separately in weak interactions with their corresponding charged leptons. This result earned Lederman, Schwartz and Steinberger the Nobel prize in 1988. The third type of neutrinos, the one associated with the τ lepton, was finally discovered in 2000 by the DONUT experiment [22].

Once different neutrino families were established the question of whether there could be mixing and transitions between them was open. The first idea of neutrino oscillations was put forward by B. Pontecorvo in 1957 [23]. In 1962 Z. Maki, M. Nakagawa and S. Sakata introduced the concept of mixing between mass and flavour states [24]. In 1967 Pontecorvo gave a first intuitive link between two neutrino mixing and oscillations [25], subsequently completed by him with V. N. Gribov two years later [26]. In

the subsequent decade the theory was fully developed [27]. On the experimental side, first indications of a transition between flavours emerged in solar neutrino experiments. Since the 60's the Homestake experiment led by R. Davies detected solar neutrinos using a radiochemical technique with chlorine [28]. In 2002 R. Davies Jr. and M. Koshiba were awarded the Nobel prize in Physics “for pioneering contributions to astrophysics, in particular for the detection of cosmic neutrinos”. Davis’ experiment observed a flux smaller than predicted by J. Bahcall and collaborators [29] in the solar neutrino model. Other radiochemical experiments Gallex/GNO [30] and Sage [31] confirmed these results. These experiments can measure neutrinos at low energies with a sub-MeV threshold but cannot reconstruct the energy or the direction of the neutrinos. Water-Cherenkov detectors, starting with Kamiokande [32], could detect solar neutrinos via elastic scattering $\nu_e e^- \rightarrow \nu_e e^-$. Their threshold is much higher making them sensitive only to the ^8B component of the flux but they can measure the energy and direction of the incoming neutrino. Super-Kamiokande was able to measure the flux deficit with great precision [33]. The solar neutrino problem remained open for a long time: whether neutrinos oscillate into flavour which cannot be detected in the experiments or the flux predictions were badly flawed. The definitive answer came in 2001 thanks to the SNO experiment [61]. It exploited two interactions in addition to elastic scattering: the charged current (CC) interaction $\nu_e + d \rightarrow p + p + e^-$ and the neutral current (NC) one $\nu_\alpha + d \rightarrow p + n + \nu_\alpha$, $\alpha = e, \mu, \tau$. The latter is particularly important as it is sensitive to all the three neutrino flavours. By comparing the ν_e and ν_α fluxes deduced from the data, the SNO experiment was able to demonstrate that ν_e constitute only roughly a third of the overall solar neutrino flux at these energies and that the observed total flux is in good agreement with the theoretical predictions. The parameters required to explain the solar neutrino transitions were confirmed by the reactor neutrino experiment KamLAND soon after in 2002 [66].

Neutrino oscillations were observed also in atmospheric neutrinos. These are produced in the atmosphere when cosmic rays interact with nuclei in the atmosphere sourcing pions and kaons, and subsequently muons, which decay producing muon and electron neutrinos. Atmospheric neutrinos were first detected in 1965 deep underground at the Kolar Gold Field Mine in India [36] and soon after in the East Rand Proprietary Gold Mine in South Africa [37] looking for upgoing muon events signaling a muon neutrino interaction. First indications of a deficit of muon neutrinos were reported by Kamiokande, IMB, Soudan2, and by MACRO [38]. In 1998, the Super-Kamiokande experiment discovered neutrino oscillations [39] showing that the muon neutrino depletion is L/E dependent in agreement with an oscillatory behaviour. We now know that muon neutrinos oscillate into tau neutrinos, which cannot be efficiently detected in the experiment. In 2015 T. Kajita for the Super-Kamiokande collaboration and A. B. McDonald for the SNO collaboration received the Nobel Prize in Physics for “*the discovery of neutrino oscillations, which shows that neutrinos have a mass*”. As we will discuss later, this is the first particle physics evidence that the SM is incomplete, see Sec. 6. Neutrino oscillations have been studied since with great precision in solar, atmospheric, accelerator, reactor neutrino experiments and a rich programme is planned for the future, see Sec. 3.3.

2 Neutrinos in the Standard Model of Particle Physics and beyond

The Standard Model of particle physics [13–15] is based on the gauge symmetry $SU(3) \times SU(2)_L \times U(1)_Y$ and categorises all known fermions via the corresponding quantum numbers. They are given in Table 1.

Neutrinos are singlets of $SU(3)$ but belong to $SU(2)_L$ doublets together with their corresponding charged leptons. They have hypercharge $-1/2$ and do not carry electric charge, as $Q = T_3 + Y$. In the SM, neutrinos are Weyl fermions with left chirality, $\nu_{\alpha L} \equiv P_L \nu_\alpha$, $\alpha = e, \mu, \tau$. The chiral projectors are $P_L = (1 - \gamma_5)/2$ and $P_R = (1 + \gamma_5)/2$. For massless neutrinos, chirality and helicity match as the chiral projectors and the projectors on helicity components are the same up to corrections of order m/E . Left-handed neutrinos are accompanied by right-handed antineutrinos as required by the invariance of the theory under CPT (charge conjugation, parity, time reversal). Parity, the transformation of left into

Table 1: SM fermionic content and its irreducible representations with respect to the groups $SU(3)$, $SU(2)_L$ and $U(1)_Y$. **3** indicates a triplet of $SU(3)$, **2** a doublet of $SU(2)_L$ and **1** a singlet with respect to either group. Y is the hypercharge of the fields.

Particles	$SU(3)$	$SU(2)_L$	$U(1)_Y$
Leptons			
$\begin{pmatrix} \nu_e \\ e \end{pmatrix}_L, \begin{pmatrix} \nu_\mu \\ \mu \end{pmatrix}_L, \begin{pmatrix} \nu_\tau \\ \tau \end{pmatrix}_L$	1	2	$-1/2$
e_R, μ_R, τ_R	1	1	-1
Quarks			
$\begin{pmatrix} u \\ d \end{pmatrix}_L, \begin{pmatrix} c \\ s \end{pmatrix}_L, \begin{pmatrix} t \\ b \end{pmatrix}_L$	3	2	$1/6$
u_R, c_R, t_R	3	1	$2/3$
d_R, s_R, b_R	3	1	$-1/3$

right and viceversa, is maximally violated in the SM as there are no right-handed neutrinos.

Left-handed neutrinos interact via the weak force according to the charged current and neutral current terms in the SM Lagrangian:

$$\mathcal{L}_{\text{SM}} = -\frac{g}{\sqrt{2}} \sum_{\alpha=e,\mu,\tau} \bar{\nu}_{\alpha L} \gamma^\mu \ell_{\alpha L} W_\mu - \frac{g}{2 \cos \theta_W} \sum_{\alpha=e,\mu,\tau} \bar{\nu}_{\alpha L} \gamma^\mu \nu_{\alpha L} Z_\mu + \text{h.c.}, \quad (2)$$

where g is the $SU(2)_L$ coupling, θ_W is the Weinberg angle, and all other symbols have the common meaning. We notice that the structure of the SM weak interaction is of the $V - A$ type.

As discussed in the Introduction, neutrinos come in three families. A fourth active neutrino is not allowed by the invisible width of the Z boson to which it would contribute as much as one active neutrino, $Z \rightarrow \nu_\alpha \bar{\nu}_\alpha$. The invisible width has been measured with great accuracy at LEP and leads to the following constraint on the active number of neutrinos [40]:

$$N_\nu = \frac{\Gamma_{inv}}{\Gamma_{\bar{\nu}\nu}} = 2.984 \pm 0.008. \quad (3)$$

Additional neutrinos could be present, as we will discuss later, but they need not partake in SM interactions, and therefore are called sterile neutrinos.

2.1 Leptonic mixing

Since neutrinos have masses, there are two bases that can be used to describe them: the flavour basis, ν_α , $\alpha = e, \mu, \tau$, depicted in Table 1, in which each neutrino is associated to the corresponding charged lepton, and the mass basis, ν_i , $i = 1, 2, 3$, in which each neutrino has a definite mass. The two bases, as required by probability conservation, are related by a unitary matrix U , the so-called Pontecorvo-Maki-Nakagawa-Sakata (PMNS) matrix [23, 24]:

$$\nu_{\alpha L} = \sum_{i=1}^3 U_{\alpha i} \nu_{iL}. \quad (4)$$

The PMNS matrix then enters the CC Lagrangian when we express it in terms of mass fields (in the basis in which the charged lepton mass matrix is diagonal):

$$\mathcal{L}_{\text{SM}} = -\frac{g}{\sqrt{2}} \sum_{\alpha,i} \bar{\nu}_i U_{\alpha i}^* \gamma^\mu P_L \ell_\alpha W_\mu + \text{h.c.}, \quad (5)$$

with $\alpha = e, \mu, \tau$ and $i = 1, 2, 3$ ²³. From here it plays a role in neutrino oscillations as we will discuss later.

In general, a 3×3 unitary matrix can be parameterized in terms of 3 angles and 6 phases. Several of the phases are unphysical. In fact, we have the freedom to phase-rotate the fields as $\psi \rightarrow e^{i\phi}\psi$. If we do so for the charged leptons, we can eliminate three phases from the PMNS matrix and these disappear from the Lagrangian as they do not affect the kinetic terms, the NC one and the mass term for the leptons as far as both left and right-handed component undergo the same rephasing. If neutrinos are Dirac particles, as the charged leptons, the same rephasing can be applied to them as well, eliminating two further phases. There remains only one physical phase, called the Dirac phase, as in the Cabibbo-Kobayashi-Maskawa mixing matrix in the quark sector. If neutrinos are Majorana, such rephasing does not eliminate two phases which will reappear in the Majorana condition and in the Majorana mass term. Therefore, for Majorana neutrinos, there are three physical phases, two of which enter only in lepton number violating processes. Since for antineutrinos we need to use the conjugate of U , any physical phase represents a violation of the CP symmetry and will be called a CP violating (CPV) phase.

The PMNS matrix can be parameterized as [41, 42]

$$U_{\alpha i} = \begin{pmatrix} c_{12}c_{13} & s_{12}c_{13} & s_{13}e^{-i\delta} \\ -s_{12}c_{23} - c_{12}s_{23}s_{13}e^{i\delta} & c_{12}c_{23} - s_{12}s_{23}s_{13}e^{i\delta} & s_{23}c_{13} \\ s_{12}s_{23} - c_{12}c_{23}s_{13}e^{i\delta} & -c_{12}s_{23} - s_{12}c_{23}s_{13}e^{i\delta} & c_{23}c_{13} \end{pmatrix} \cdot \mathcal{P}, \quad (6)$$

where we define $c_{ij} \equiv \cos \theta_{ij}$ and $s_{ij} \equiv \sin \theta_{ij}$, with $\theta_{ij} \in [0, 90^\circ]$. In this notation, δ is the Dirac CPV phase $\delta \in [0, 360^\circ]$ and \mathcal{P} is a diagonal phase matrix $\mathcal{P} \equiv \text{diag}(1, e^{i\frac{\alpha_{21}}{2}}, e^{i\frac{\alpha_{31}}{2}})$ which embeds the two Majorana CPV phases α_{21}, α_{31} .

It is interesting to express the CP-violating effects due to the Dirac phase in a rephasing-invariant manner. This can be done using the Jarlskog invariant [43]

$$J \equiv \Im[U_{\mu 3}U_{e 2}U_{\mu 2}^*U_{e 3}^*] = \frac{1}{8} \sin 2\theta_{12} \sin 2\theta_{23} \sin 2\theta_{13} \cos \theta_{13} \sin \delta. \quad (7)$$

This formulation makes apparent that Dirac CP violation is a genuine 3-neutrino mixing effect whose physical impact depends on all of the three mixing angles, including the relatively small θ_{13} .

3 Neutrino oscillations

In presence of leptonic mixing and non-degenerate neutrino masses, the phenomenon of neutrino oscillations takes place. This is a beautiful manifestation of quantum mechanics on macroscopic distances. The basic picture is the following. In production and detection neutrinos are described by flavour states. Let's assume that a muon neutrino is produced. This is a coherent superposition of massive states which have slightly different masses. The *coherence* is a key condition which needs to be satisfied to have neutrino oscillations. It is satisfied thanks to the uncertainty in the neutrino momentum at production⁴. The massive components of the initial state propagate over long distances with slightly different phases. This amounts to a change in the state over distance. It is then possible that at detection, when projecting the flavour components out, a different flavour is found compared to the initial one. In order for the oscillatory behaviour to hold, coherence is needed also during propagation and this is possible because of the very weakly interacting nature of neutrinos⁵.

²Unless otherwise indicated, we will use Greek indexes for flavour fields/states and Roman ones for mass fields/states.

³The flavour states are related to mass states as $|\nu_\alpha\rangle = \sum_i U_{\alpha i}^* |\nu_i\rangle$.

⁴If the momentum uncertainty is small compared to the mass differences, for instance if there exists a very heavy nearly-sterile neutrino, such coherence is lost and oscillations do not develop. At production in a specific event either the light states will be produced coherently or the heavy one.

⁵Over astronomical distances the massive components of neutrinos can separate in the wave function due to the slightly different velocities, effectively destroying coherence.

3.1 Oscillation probability in vacuum

The oscillation probability can be derived in different ways but here we will limit the discussion to the commonly used plane-wave approximation. This approximation does not capture the momentum uncertainty necessary for coherence. We will assume by hand that the initial state is a coherent superposition of massive states with a definite spatial momentum $p \equiv |\mathbf{p}|$.

Let's consider a ν_α produced at $t = 0$ in a charged current interaction. We describe the initial state as a superposition of mass eigenstates, which we take as plane waves with momentum p ,

$$|\nu, t = 0\rangle = |\nu_\alpha\rangle = \sum_i U_{\alpha i}^* |\nu_i\rangle. \quad (8)$$

The mass states $|\nu_i\rangle$ are eigenstates of the free Hamiltonian \hat{H} with eigenvalues $E_i = \sqrt{\mathbf{p}^2 + m_i^2}$. The evolution of the neutrino state can be obtained by solving the evolution equation and is expressed as⁶

$$|\nu, t\rangle = \exp(-i\hat{H}t)|\nu_\alpha\rangle = \sum_i U_{\alpha i}^* \exp(-iE_i t) |\nu_i\rangle. \quad (9)$$

The probability of transition from ν_α to ν_β at time t is obtained projecting the state $|\nu, t\rangle$ in the ν_β direction as

$$P(\nu_\alpha \rightarrow \nu_\beta, t) = |\langle \nu_\beta | \nu, t \rangle|^2 = \left| \sum_i U_{\beta i} U_{\alpha i}^* \exp(-iE_i t) \right|^2, \quad (10)$$

where we have used the fact that $\langle \nu_j | \nu_i \rangle = \delta_{ij}$.

In all experimentally relevant situations, neutrinos are highly relativistic and one can approximate, for common momentum p ,

$$E_i - E_j \simeq \frac{m_i^2 - m_j^2}{2p}, \quad (11)$$

and moreover one can take $L = t$.

Finally, one obtains the general formula for neutrino oscillations in vacuum

$$P(\nu_\alpha \rightarrow \nu_\beta, t) = |\langle \nu_\beta | \nu, t \rangle|^2 = \left| \sum_i U_{\beta i} U_{\alpha i}^* \exp\left(-i \frac{\Delta m_{i1}^2 t}{2E}\right) \right|^2, \quad (12)$$

where we have defined $\Delta m_{i1}^2 \equiv m_i^2 - m_1^2$ and we have approximated $E \simeq p$. It is apparent from this formula that oscillations between one flavour and another are possible only if there is leptonic mixing, $U \neq 1$, and neutrinos have masses. This is the reason why the discovery of neutrino oscillations in 1998 has had such a groundbreaking effect in our understanding of neutrinos and more broadly of particle physics.

We notice that neutrino oscillations conserve lepton number, i.e. if a neutrino is produced, the state will continue being a neutrino, but does not respect leptonic flavour as the neutrino can change from one to the other over distances. We furthermore notice that Majorana phases do not enter in the oscillation formula as expected since this is a lepton number conserving process. Moreover, the overall mass scale does not play a role in it.

The case $\alpha = \beta$ is usually referred to as a survival probability or disappearance channel, the opposite one $\alpha \neq \beta$ is the transition probability or appearance channel. Conservation of probability is satisfied as $\sum_\beta P(\nu_\alpha \rightarrow \nu_\beta, t) = 1$. For antineutrinos, one substitutes U with its complex conjugate U^* .

⁶We use natural units throughout: $c = 1, \hbar = 1$.

It is sometimes useful to separate the real and imaginary parts of the leptonic mixing terms as

$$P(\nu_\alpha \rightarrow \nu_\beta) = \delta_{\alpha\beta} - 4 \sum_{i>j} \Re[U_{\alpha i}^* U_{\alpha j} U_{\beta j}^* U_{\beta i}] \sin^2 \left(\frac{\Delta m_{ij}^2 L}{4E} \right) + 2 \sum_{i>j} \Im[U_{\alpha i}^* U_{\alpha j} U_{\beta j}^* U_{\beta i}] \sin \left(\frac{\Delta m_{ij}^2 L}{2E} \right). \quad (13)$$

The plane-wave derivation we have discussed above has the advantage of simplicity but cannot account for the momentum uncertainty necessary for coherence and the spatial size of the neutrino wave function resulting from the fact that production and detection are localised processes. A more precise treatment of this problem has been achieved using wave packets so that the initial state is the superposition of the wave packets which describe each massive neutrino [44]. This derivation allows to incorporate decoherence and momentum uncertainty effects. The approximation $L = t$ is also problematic in the plane-wave description as plane waves extend all over the space with the same amplitude. The wave packets can describe localised particles and solve this apparent paradox as well. In all experimentally relevant cases, it will result in the same formula as Eq. (12) as far as coherence is maintained and the momentum uncertainty is sufficiently large. For further details about this derivation and a discussion of neutrino oscillations in the context of QFT, see e.g. [45].

3.1.1 2-neutrino oscillations

We now study the probability in Eq. (12) more in detail [26, 27]. Let's consider first the oscillation probability in the two neutrino case. The massive basis ν_1, ν_2 is related to the flavour basis ν_α, ν_β as

$$\begin{pmatrix} \nu_\alpha \\ \nu_\beta \end{pmatrix} = \begin{pmatrix} \cos \theta & \sin \theta \\ -\sin \theta & \cos \theta \end{pmatrix} \begin{pmatrix} \nu_1 \\ \nu_2 \end{pmatrix}, \quad (14)$$

where θ is the mixing angle in vacuum which parameterizes the 2×2 mixing matrix.

The oscillation appearance probability is given by

$$P(\nu_\alpha \rightarrow \nu_\beta) = \sin^2 2\theta \sin^2 \left(\frac{\Delta m^2 L}{4E} \right). \quad (15)$$

We schematically show $P(\nu_\mu \rightarrow \nu_\tau)$ in Fig. 1.

As expected, we see that this probability is different from zero only in presence of mixing and of neutrino masses. Oscillations do not develop if the distance travelled by the neutrinos is too short and they reach a maximum when $\frac{\Delta m^2 L}{4E} = \pi/2$. For a given baseline, set by the distance between the source and the detector, the energy of the first oscillation maximum is controlled by Δm^2 . It is useful to express the argument in terms of experimentally relevant units as

$$\frac{\Delta m^2 L}{4E} = 1.27 \frac{\Delta m^2}{\text{eV}^2} \frac{L}{\text{km}} \frac{\text{GeV}}{E}. \quad (16)$$

The disappearance probability $P(\nu_\alpha \rightarrow \nu_\alpha)$ is simply $1 - P(\nu_\alpha \rightarrow \nu_\beta)$. We also notice that CPT invariance guarantees that $P(\nu_\alpha \rightarrow \nu_\beta) = P(\bar{\nu}_\beta \rightarrow \bar{\nu}_\alpha)$ and that the disappearance probability is the same for neutrinos and antineutrinos $P(\nu_\alpha \rightarrow \nu_\alpha) = P(\bar{\nu}_\alpha \rightarrow \bar{\nu}_\alpha)$. Moreover, we have that the probability is invariant under a T and CP transformations, since $P(\nu_\alpha \rightarrow \nu_\beta) = P(\nu_\beta \rightarrow \nu_\alpha) = P(\bar{\nu}_\alpha \rightarrow \bar{\nu}_\beta)$. This implies that 2-neutrino oscillations in vacuum are not sensitive to leptonic CP violation and therefore to hunt for the Dirac CPV phase it is necessary to exploit setups for which 3-neutrino oscillation effects are relevant.

3.1.2 3-neutrino oscillations

In the case of 3-neutrino mixing, the probability of $\nu_\alpha \rightarrow \nu_\beta$ oscillations in vacuum has a more complex form in terms of the two mass squared differences Δm_{21}^2 and Δm_{31}^2 and of the mixing parameters. In experimental situations, two limits are particularly interesting.

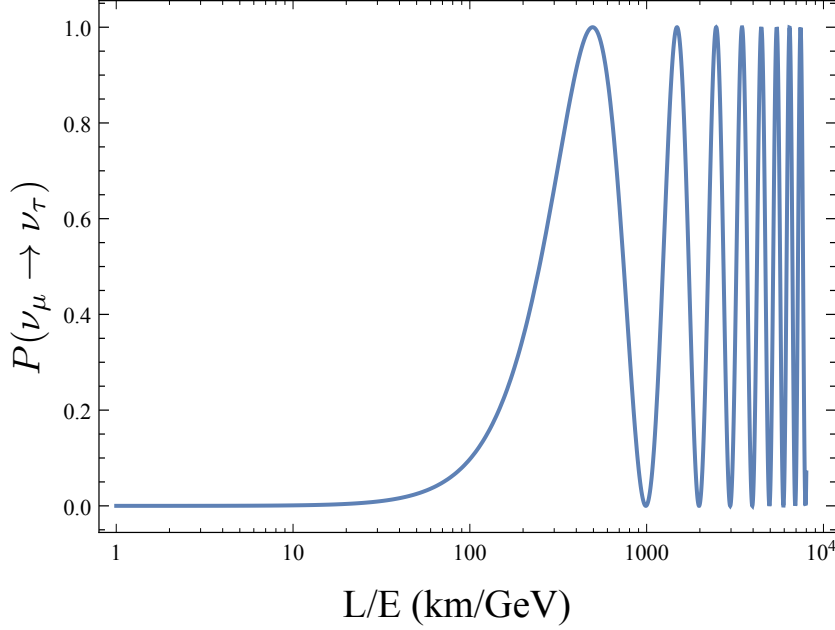


Fig. 1: The transition probability $P(\nu_\mu \rightarrow \nu_\tau)$ in the 2-neutrino mixing approximation as a function of L/E for $\sin^2 2\theta = 1$ and $\Delta m^2 = 2.5 \times 10^{-3} \text{ eV}^2$.

- Case A: $\frac{\Delta m_{21}^2 L}{2E} \ll 1$. This is the case relevant for accelerator, atmospheric, and medium baseline reactor neutrino experiments as far as subdominant 3-neutrino mixing effects can be neglected. The oscillations due to Δm_{21}^2 do not develop and the probability reduces to:

$$P(\nu_\alpha \rightarrow \nu_\beta) \simeq 4|U_{\alpha 3}|^2|U_{\beta 3}|^2 \sin^2 \left(\frac{\Delta m_{31}^2 L}{4E} \right). \quad (17)$$

This formula resembles the one for the 2-neutrino oscillation case and indeed has the same properties, in that it is not sensitive to CP-violating effects.

Accelerator neutrino experiments such as T2K and NOvA, and in the past MINOS, K2K, and atmospheric neutrino experiments, specifically Super-Kamiokande, exploit a muon neutrino beam, mainly from pion decays and can measure quite precisely its disappearance probability given by

$$P(\nu_\mu \rightarrow \nu_\mu) \simeq 1 - 4|U_{\mu 3}|^2(1 - |U_{\mu 3}|^2) \sin^2 \left(\frac{\Delta m_{31}^2 L}{4E} \right) \simeq 1 - \sin^2 2\theta_{23} \sin^2 \left(\frac{\Delta m_{31}^2 L}{4E} \right) + \mathcal{O}(s_{13}^2). \quad (18)$$

Consequently, they provide the dominant information on Δm_{31}^2 and on the θ_{23} angle. The current generation experiments T2K and NOvA are also designed to detect electron neutrinos from the $\nu_\mu \rightarrow \nu_e$ oscillations at long distance. The probability at leading order is given by

$$P(\nu_\mu \rightarrow \nu_e) \simeq 4|U_{e 3}|^2|U_{\mu 3}|^2 \sin^2 \left(\frac{\Delta m_{31}^2 L}{4E} \right) \simeq s_{23}^2 \sin^2 2\theta_{13} \sin^2 \left(\frac{\Delta m_{31}^2 L}{4E} \right). \quad (19)$$

We note that this probability is suppressed by the small mixing angle θ_{13} . Subdominant terms arise due to matter effects, see Sec. 3.2, and Dirac CP violation. This is the channel of choice to determine the mass ordering and discover CP violation in long baseline neutrino oscillation experiments.

Finally, the probability which is relevant for medium baselines $L \sim 1 \text{ km}$ in reactor neutrino experiments is

$$P(\bar{\nu}_e \rightarrow \bar{\nu}_e) \simeq 1 - \sin^2 2\theta_{13} \sin^2 \left(\frac{\Delta m_{31}^2 L}{4E} \right). \quad (20)$$

This probability is controlled again by θ_{13} and, thanks to this, the Daya Bay experiment [46], as well as RENO [47] and Double CHOOZ [48], discovered $\theta_{13} \neq 0$ in 2012.

- Case B: $\frac{\Delta m_{31}^2 L}{2E} \gg 1$. Long baseline reactor neutrino experiments such as KamLAND exploit this approximation. In this case, the oscillations controlled by Δm_{31}^2 are effectively averaged out. The probability can be well approximated by

$$P(\bar{\nu}_e \rightarrow \bar{\nu}_e) \simeq c_{13}^2 \left[1 - \sin^2 2\theta_{12} \sin^2 \left(\frac{\Delta m_{21}^2 L}{4E} \right) \right] + s_{13}^2. \quad (21)$$

It follows that KamLAND can measure very precisely the value of Δm_{21}^2 and is sensitive to θ_{12} and at some level also to θ_{13} [49].

If 3-neutrino mixing effects are at play, the neutrino probability becomes sensitive to Dirac CP violation. This can be seen computing the CP asymmetry $\mathcal{A}(\nu_\alpha \rightarrow \nu_\beta) \equiv P(\nu_\alpha \rightarrow \nu_\beta) - P(\bar{\nu}_\alpha \rightarrow \bar{\nu}_\beta)$. Using Eq. (13) it follows that

$$\mathcal{A}(\nu_\alpha \rightarrow \nu_\beta) = 4s_{12}c_{12}s_{13}c_{13}^2s_{23}c_{23} \sin \delta \left[\sin \left(\frac{\Delta m_{21}^2 L}{4E} \right) + \sin \left(\frac{\Delta m_{13}^2 L}{4E} \right) + \sin \left(\frac{\Delta m_{32}^2 L}{4E} \right) \right]. \quad (22)$$

We notice that CPV effects can be parameterised in terms of the Jarlskog invariant and depend on the Dirac CPV phase. Moreover, they are different from zero only in presence of 3-neutrino oscillation effects, i.e. if Δm_{21}^2 can be neglected $\mathcal{A}(\nu_\alpha \rightarrow \nu_\beta)$ goes to zero. This implies that CPV effects are suppressed by the small mass squared difference Δm_{21}^2 and are controlled by the small mixing angle θ_{13} making their search challenging. Current long baseline neutrino oscillation experiments have started being sensitive to these effects which are the main focus of next generation experiments.

3.2 Matter effects in neutrino oscillations

Neutrinos are affected by the medium in which they travel. They can incoherently scatter off its components, e.g. electrons, neutrons, protons, but typically these interactions can be neglected. Using dimensional arguments, a crude estimate of the interaction cross section for a neutrino of energy E is

$$\sigma_\nu \sim G_F^2 EM \sim 10^{-38} \text{ cm}^2 \frac{EM}{\text{GeV}^2},$$

where we have used a mass M for the target in the medium, typically being nucleons. Considering for instance the Earth density this cross section leads to a mean free path of 10^{14} cm at 1 GeV, well above the Earth diameter. Indeed the Earth becomes opaque to neutrinos only at energies above 10^2 TeV. Only in extremely dense environments, such as supernovae cores and the Early Universe, these interactions are sufficiently frequent to trap the neutrinos.

In the low density situations of interest, e.g. the Earth and the Sun, the medium affects neutrinos nevertheless by modifying their effective masses. In matter, neutrinos interact with the background particles, e.g. electrons, protons and neutrons, via forward elastic scattering [50]. Let's consider a neutral unpolarised medium at rest. We consider centre-of-mass energies well below the W and Z masses, for which we can use the Fermi approximation. The effective Hamiltonian density for the CC interaction is given by

$$H_{CC} = 2\sqrt{2}G_F[\bar{e}\gamma_\mu P_L\nu_e][\bar{\nu}_e\gamma^\mu P_L e] = 2\sqrt{2}G_F[\bar{\nu}_e\gamma^\mu P_L\nu_e][\bar{e}\gamma_\mu P_L e], \quad (23)$$

where we have used a Fierz transformation to separate the neutrino part from the background electron one. Averaging the electron component over the background at rest gives

$$\langle \bar{e}\gamma_\mu P_L e \rangle = \delta_{\mu 0} \frac{N_e}{2}, \quad (24)$$

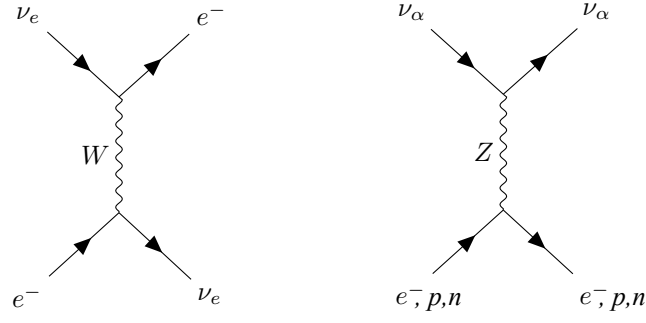


Fig. 2: Feynman diagrams for the CC and NC neutrino interactions with a medium, such as the Earth or the Sun.

where N_e is the electron density. Similarly, one can compute the contribution due to the NC interactions. In this case, in a neutral background, the electron and proton contributions cancel out and only the neutron density N_n is relevant.

By considering the modified dispersion relations in matter, one can see that an effective potential is induced in the Hamiltonian:

$$V_e = \sqrt{2}G_F \left(N_e - \frac{N_n}{2} \right), \quad (25)$$

$$V_{\mu,\tau} = \sqrt{2}G_F \left(-\frac{N_n}{2} \right). \quad (26)$$

For antineutrinos the potential changes sign. This indicates a violation of CP and CPT symmetries, which is due to the fact that the background is itself CP and CPT violating as it contains only particles and not antiparticles⁷.

Notice that these terms are diagonal in the flavour basis as there are no SM processes which change one flavour into another and that the NC terms are the same for all three flavours as NC interactions are flavour blind in the SM.

The effective Hamiltonian, describing the neutrino propagation in the medium, is given by the vacuum one H^0 augmented by the potential terms as

$$H^m = H^0 + \text{diag}(V_e, V_\mu, V_\tau), \quad (27)$$

in the flavour basis.

Let's consider the simplest case of 2-neutrino oscillations and choose the ν_e - ν_μ flavours⁸. In the flavour basis the neutrino propagation can be described by

$$i \frac{d}{dt} \begin{pmatrix} \nu_e \\ \nu_\mu \end{pmatrix} = \begin{pmatrix} -\frac{\Delta m^2}{4E} \cos 2\theta_o + \sqrt{2}G_F N_e(t) & \frac{\Delta m^2}{4E} \sin 2\theta_o \\ \frac{\Delta m^2}{4E} \sin 2\theta_o & \frac{\Delta m^2}{4E} \cos 2\theta_o \end{pmatrix} \begin{pmatrix} \nu_e \\ \nu_\mu \end{pmatrix}. \quad (28)$$

For clarity we have indicated the mixing angle in vacuum as θ_o and it corresponds to θ in Eq. 14. To derive this expression we have eliminated any common term in the diagonal as only relative phases between the states are relevant in the probabilities. Computing the resulting evolution can be highly non trivial, especially in the full 3-neutrino mixing picture, and one may have to resort to numerical tools. In some case, analytical approximations can be applied. We consider two particularly relevant ones: the constant density case and the case of varying density with adiabaticity.

⁷This is not the case in the Early Universe in which both types are typically present with a very similar density.

⁸As the matter potential is the same for ν_μ and ν_τ , we do not expect matter effects to arise in the oscillations between these two flavours, at least at leading order.

3.2.1 Constant density case

For constant density, the evolution of the two eigenstates in matter can be decoupled. The mixing between the flavour states and the eigenstates in matter is

$$\tan 2\theta_m = \frac{\frac{\Delta m^2}{2E} \sin 2\theta_o}{\frac{\Delta m^2}{2E} \cos 2\theta_o - \sqrt{2}G_F N_e}. \quad (29)$$

The probability of oscillation can be computed in analogy to the vacuum case and is given by

$$P(\nu_e \rightarrow \nu_\mu; t) = \sin^2 2\theta_m \sin^2 \left(\frac{L}{2} (E_A - E_B) \right), \quad (30)$$

with

$$|E_A - E_B| = \sqrt{\left(\frac{\Delta m^2}{2E} \cos 2\theta_o - \sqrt{2}G_F N_e \right)^2 + \left(\frac{\Delta m^2}{2E} \sin 2\theta_o \right)^2}. \quad (31)$$

We notice that the behaviour in matter can be significantly different to the vacuum case [51].

- *Vacuum limit.* If $\sqrt{2}G_F N_e \ll \frac{\Delta m^2}{2E} \cos 2\theta_o$, $\theta_m \simeq \theta_o$ and the vacuum solution is recovered.
- *Matter domination.* If $\sqrt{2}G_F N_e \gg \frac{\Delta m^2}{2E} \cos 2\theta_o$, matter effects dominate and the transition probability is very suppressed. This can be understood as matter effects are flavour diagonal and therefore tend to realign the evolving state onto the initial flavour direction, suppressing flavour transitions.
- *Resonance.* The remaining option is particularly interesting and happens when $\sqrt{2}G_F N_e = \frac{\Delta m^2}{2E} \cos 2\theta_o$. In this case the mixing angle in matter is maximal, $\theta_m = \pi/4$, independently from the value of θ_o . This case is called "resonance" and can happen for neutrinos (antineutrinos) if $\Delta m^2 > 0$ ($\Delta m^2 < 0$), for $\cos 2\theta_o > 0$. Once the resonant condition is satisfied, the oscillation length is controlled by $|E_A - E_B| = \frac{|\Delta m^2|}{2E} \sin 2\theta_o$ requiring very long distances for the oscillations to develop if θ_o is very small.

The case of constant density is relevant for long baseline neutrino oscillations experiments, e.g. NOvA, DUNE. By searching for an enhancement of the oscillation probability in neutrinos or antineutrinos due to matter effects, these experiments are sensitive to the sign of Δm_{31}^2 , or the mass ordering. These are typically small effects and are partly degenerate with intrinsic CPV effects due to the Dirac phase, which are also opposite for neutrinos and antineutrinos. Focusing on the $\nu_\mu \rightarrow \nu_e$ transition, an approximate form of the oscillation probability allows to study the dependence on the various effects [52]

$$P(\nu_\mu \rightarrow \nu_e) \simeq s_{23}^2 \sin^2 2\theta_{13} \left(\frac{\Delta_{31}}{\Delta_{31} \mp A} \right)^2 \sin^2 \frac{(\Delta_{31} \mp A)L}{2} + c_{13} \sin 2\theta_{13} \sin 2\theta_{12} \sin \theta_{23} \frac{\Delta_{21}}{A} \sin \frac{AL}{2} \frac{\Delta_{31}}{|\Delta_{31} \mp A|} \sin \frac{|\Delta_{31} \pm A|L}{2} \cos \left(\frac{\Delta_{31}L}{2} \mp \delta \right) + \mathcal{O}(\Delta_{12}^2 L), \quad (32)$$

with $\Delta_{ij} \equiv \Delta m_{ij}^2/2E_\nu$ and $A \equiv V_e - V_\mu = \sqrt{2}G_F N_e$. Due to the fact that θ_{13} is not too small, see Sec. 3.4, the first term dominates and provides sensitivity to matter effects and the mass ordering. The second term in this expression depends on the CPV phase δ . As expected, it arises from the interference of the oscillations due to both Δm_{31}^2 and Δm_{21}^2 and increases at lower energies. From this expression, we can understand that determining the mass ordering and CPV in long baseline neutrino oscillation experiments is possible but presents some challenges. Having information at different energies and both for neutrinos and antineutrinos alleviates the degeneracy between the various parameters and enhances the physics reach.

3.2.2 Varying density

In many situations, the neutrinos travel through a medium of varying density. This is the case for neutrinos produced in the inner parts of the Sun or for atmospheric neutrinos going through the Earth.

At any given time, it is possible to diagonalise the Hamiltonian and find the corresponding instantaneous propagation states, ν_A, ν_B . The mixing angle in matter is time dependent as its expression depends on the local density. As a result, in this basis, the Hamiltonian acquires off-diagonal terms which depend on the time derivative of the potential as

$$i \frac{d}{dt} \begin{pmatrix} \nu_A \\ \nu_B \end{pmatrix} = \begin{pmatrix} E_A & -i\theta_m(t) \\ i\theta_m(t) & E_B \end{pmatrix} \begin{pmatrix} \nu_A \\ \nu_B \end{pmatrix}. \quad (33)$$

For constant density, the off-diagonal terms are zero and the two states ν_A and ν_B evolve independently. For varying density, the off-diagonal terms indicate the possibility of a transition from one state to the other. An analytical solution is typically very difficult to obtain and numerical tools need to be employed to compute the transition probabilities. If the off-diagonal terms are subdominant, as it happens for a slowly varying density, then some approximate solution can be found. This is the adiabatic case for which the adiabatic condition is satisfied

$$|E_A - E_B| \gg \left| \frac{d}{dt} \theta_m \right|. \quad (34)$$

The case of varying density is realised in the Sun, in which the neutrinos see a slowly varying density as they travel towards the surface. Let's consider the 2-neutrino mixing approximation. At any time t , it is possible to relate the flavour states to the instantaneous propagation states. Explicitly we have

$$\begin{pmatrix} \nu_e \\ \nu_\mu \end{pmatrix} = \begin{pmatrix} \cos \theta_m(t) & \sin \theta_m(t) \\ -\sin \theta_m(t) & \cos \theta_m(t) \end{pmatrix} \begin{pmatrix} \nu_A \\ \nu_B \end{pmatrix}. \quad (35)$$

As neutrinos originate from close to the centre of the Sun, at sufficiently high energies, matter effects dominate and $\theta_m \sim \pi/2$ implying that electron neutrinos are mainly in the heavy state ν_B . This can be seen from the form of the Hamiltonian in Eq. (28) which is nearly diagonal with the dominant term in the ee position. As neutrinos reach the surface, they have remained in the same state ν_B as far as the adiabaticity condition is satisfied. At this position, the vacuum case applies so that $\theta_m = \theta_o$ and

$$|\nu_B\rangle = \sin \theta_o |\nu_e\rangle + \cos \theta_o |\nu_\mu\rangle, \quad (36)$$

implying that the survival probability is

$$P(\nu_e \rightarrow \nu_e, \text{surface}) = \sin^2 \theta_o. \quad (37)$$

If the mixing angle in vacuum is small, this corresponds to a nearly total transition to ν_μ . This is the so-called MSW effect [50, 51] and explains neutrino transitions in the Sun for energies of few MeV. It should be noted that it is improper to speak about oscillations for these transitions. In fact the survival probability does not result from the coherent evolution of the mass eigenstates produced at the source but by the independent evolution of the propagation states, so that, at these energies, most solar neutrinos we observe on the Earth are mass eigenstates ν_2 .

At low energies, matter effects are always negligible and vacuum oscillations take place, averaged over the long distances. This produces a very typical transition behaviour, with the probability at low energies given by $P(\nu_e \rightarrow \nu_e, \text{surface}) = 1 - 1/2 \sin^2 2\theta_o$, a transition region around the few MeV and $P(\nu_e \rightarrow \nu_e) = \sin^2 \theta_o$ at high energies. The dependence on neutrino masses arises from the energy at which the resonant condition is satisfied. In Fig. 3 we schematically show the behaviour of the solar neutrino survival probability.

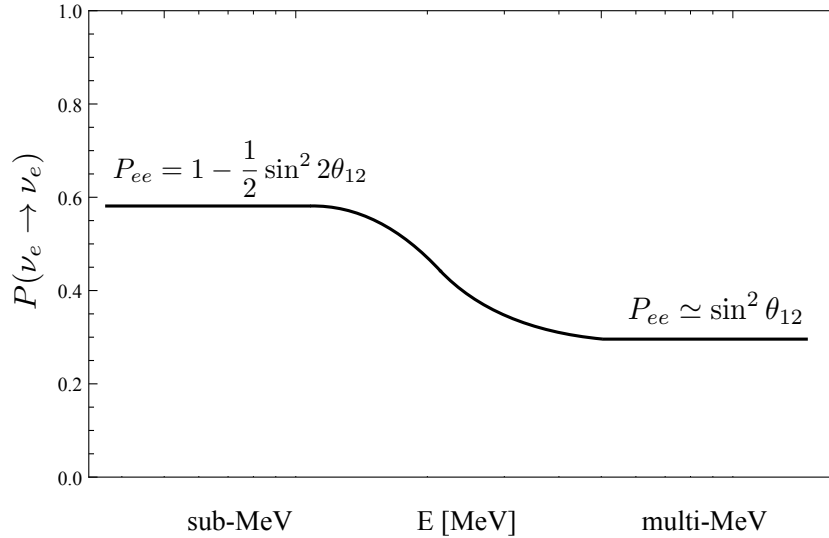


Fig. 3: A schematic representation of the electron neutrino survival probability $P(\nu_e \rightarrow \nu_e)$ for solar neutrinos, as a function of the energy.

3.3 Experimental knowledge on neutrino oscillations

Since the discovery of neutrino oscillations, a rather precise picture of neutrino oscillation properties has been painted by a very rich experimental programme. Neutrino oscillations have been observed in atmospheric, accelerator, solar, reactor neutrino experiments. Here, we provide a very concise summary, referring the reader to more updated and broad discussions available in the literature and in conferences.

3.3.1 Atmospheric neutrinos

Neutrinos are produced in the atmosphere by pion and kaon decays, and subsequent muon decays, produced by cosmic rays hitting the atmosphere. The flux is mainly made of muon neutrinos and electron neutrinos with a ratio of two since there are two muon neutrinos, one coming from pion decay and one from muon decay, per electron neutrino⁹. The spectrum is very broad going from sub-GeV to multi-TeV energies. For neutrino oscillation purposes the range of interest spans from hundreds of MeV to a few GeV.

Since the discovery of neutrino oscillations in atmospheric neutrinos by the Super-Kamiokande experiment, several experiments have studied these oscillations in greater detail. Super-Kamiokande 1-4 has collected more data [53], MINOS [54] has been able to distinguish neutrinos from antineutrinos, thanks to its magnetisation, and IceCube/DeepCore have also provided relevant information [55].

Atmospheric neutrinos contribute to our current knowledge of neutrino parameters mainly by observing the muon neutrino disappearance channel. This gives information on Δm_{31}^2 and the angle θ_{23} , see Eq. (18). Thanks to the strong matter effects, some information can also be obtained on the mass ordering, although the lack of magnetisation of the Super-Kamiokande detector and the limited number of events do not allow to reach a high statistical significance.

3.3.2 Accelerator neutrinos

Accelerator neutrinos are produced in the similar manner as atmospheric neutrinos, by focusing a pion beam down a decay pipe. This allows to have a controlled beam, in which the electron neutrino compo-

⁹At high energy this ratio becomes much bigger as muons hit the Earth before decaying, so that the electron component is suppressed.

ment is suppressed, the spectrum can be predicted with good accuracy, the intensity is enhanced and the average energy tuned to match the first oscillation maximum.

After K2K, several experiments took place including MINOS [54, 56], and the currently running T2K [57] and NOvA [58]. MINOS [54, 56] used the NuMI (Neutrinos at Main Injector) beam sourced at Fermilab and two iron magnetised detectors made of alternating planes of steel and plastic scintillators. The near detector, with a mass of 980 tons, was close to the beam target. The far detector was located in the Soudan mine in Northern Minnesota, 735 km from Fermilab, and had a mass of 5.4 ktons. Being made of magnetised steel these detectors had very good muon reconstruction capabilities and could distinguish neutrinos from antineutrino events. T2K (Tokai-to-Kamioka) experiment [57] exploits a beam produced at the J-PARC facility and the Super-Kamiokande detector located 295 km away. Due to its position, the beam reaching the detector is off-axis, resulting in a beam peaked at lower energies compared with the on-axis one. This is useful as it reduces the backgrounds due to the high energy tail of the neutrinos and increases the number of events at the first oscillation maximum. The Water-Cherenkov detector allows to reconstruct both muon and electron neutrino events. The NOvA experiment [58] also aims at detecting electron neutrinos, as well as muon ones, from the NuMI beam. The 14 kton detector is at Ash River in Minnesota 810 km from Fermilab and is made of cells of plastic PVC filled with liquid scintillator. Also in this experiment, the location is off-axis.

All these experiments provide key information on Δm_{31}^2 and the angle θ_{23} , thanks to their ability to measure the muon neutrino survival probability. T2K and NOvA are also aimed at detecting the $\nu_\mu \rightarrow \nu_e$ transition channel whose probability depends on θ_{13} and subdominantly on the CPV Dirac phase δ . NOvA, thanks to its rather long baseline of ~ 810 km, has also some sensitivity to the mass ordering via matter effects.

We should also mention the OPERA experiment, which detected ν_τ from oscillations of the CNGS beam sourced at CERN [59]. It was located at the Gran Sasso Laboratories 735 km away. The detector was made of lead bricks and nuclear emulsions, to search for the characteristic tau tracks. It was able to observe 5 tau neutrino events, confirming the hypothesis of $\nu_\mu \rightarrow \nu_\tau$ oscillations.

3.3.3 Solar neutrinos

Solar electron neutrinos are produced in the nuclear reactions that burn hydrogen into helium in the Sun, and all other stars:



A multicomponent flux is generated: pp neutrinos dominate but have rather low energies, $E_\nu \lesssim 0.4$ MeV, ${}^8\text{B}$ neutrinos have much higher energies reaching above 10 MeV although with a much lower flux, ${}^7\text{Be}$ and pep neutrinos have monochromatic lines at intermediate energies.

In recent years solar neutrinos have been studied mainly with the Super-Kamiokande detector [60], via the elastic scattering process $\nu_e e \rightarrow \nu_e e$, with SNO [61], sensitive to both electron neutrino and the overall flux as discussed earlier, and more recently with Borexino [62], which thanks to its low threshold can detect ${}^7\text{Be}$ and pep neutrinos. These experiments provide information on the mixing angle θ_{12} and, by reconstructing the transition probability above and below the resonance, on Δm_{21}^2 . As discussed in Sec. 3.2, the resonance condition depends on Δm_{21}^2 whose value can be then extracted with some level of precision. By observing the resonant behaviour for neutrinos, we can also deduce that Δm_{21}^2 is positive, for $\cos 2\theta_{12} > 0$, establishing the hierarchy between m_1 and m_2 .

3.3.4 Reactor neutrinos

After the Reines and Cowan experiment, many other reactor neutrino experiments have taken place using reactor electron anti-neutrinos. Depending on the distance, we can classify them as short¹⁰, for

¹⁰We will refer to reactor neutrino experiments searching for sterile neutrinos using baselines of tens of meters as "very-short" baseline experiments.

$L \sim 1$ km, intermediate, for $L \sim 50\text{--}60$ km, or long baseline, for $L > 100$ km, ones. Short-baseline experiments have a detector located typically around 1 km from the nuclear core. This is the case for currently running Daya Bay [46,63], RENO [47,64] and Double CHOOZ [48,65]. By exploiting inverse beta decays, they search for electron antineutrino disappearance. As shown in Eq. (20), this depends on θ_{13} which has been found to be non-zero in 2012 by these experiments, after previous hints and some clear indications by T2K.

The long baseline KamLAND experiment [66], a 1 kton liquid scintillator detector, observed neutrinos coming from all nuclear reactors in Japan, with an average distance of 175 km. At these baselines, the oscillation expression in Eq. (21) applies showing that this experiment provides the most precise information on Δm_{21}^2 as well as a measurement of θ_{12} [49,66]. Remarkably, the solar neutrino oscillations and KamLAND results pointed to the same values of these parameters.

3.3.5 Short baseline neutrino oscillations

Although we focus on the 3-neutrino mixing scenario, we mention here that neutrino oscillation experiments at short baselines have reported some hints which can be interpreted as being due to light sterile neutrinos. In the 90s the LSND experiment found evidence of $\bar{\nu}_\mu \rightarrow \bar{\nu}_e$ transitions using muon antineutrinos from pion decays [67]. This result could be explained with neutrino oscillations at very short baseline induced by a large mass squared difference $\Delta m^2 \sim 1 \text{ eV}^2$. In order to accommodate such large value together with the measured $\Delta m_{31}^2 \simeq 2.5 \times 10^{-3} \text{ eV}^2$ and $\Delta m_{21}^2 \simeq 8 \times 10^{-5} \text{ eV}^2$, it is necessary to introduce 4 massive neutrinos. The fourth flavour state needs not to have SM interactions as implied by the Z invisible width, see Eq. (3), hence the name of sterile. The MiniBooNE experiment, designed to test this result, observed some anomaly as well, namely an excess of electron neutrino events at low energies [68]. The LSND and MiniBooNE results could be interpreted in terms of neutrino oscillations, see also Ref. [70]¹¹. These results are somewhat in tension with disappearance experiments, driven mainly by MINOS+ and IceCube, which put very stringent constraints on the mixing between the muon and the fourth massive neutrinos [70], disfavouring this explanation. Regarding the mixing with electron neutrinos, there are some additional indications in favour of sterile neutrinos. Very short baseline reactor neutrino experiments, with $L \sim \text{few m}$, have measured a flux which is lower than predicted by $\sim 3\%$ [71]. Although there are significant uncertainties on the reactor neutrino flux computations, these results could be regarded in favour of sterile neutrino oscillations with $|U_{e4}|^2 \sim 0.01$. The Gallium anomaly refers to a deficit of measured electron neutrinos from radioactive sources at the GALLEX and SAGE solar neutrino experiments [72], calling for a somewhat larger value of the mixing angle $|U_{e4}|^2 \sim 0.1$.

A coherent picture is still missing and several experiments are taking data. The SBN (Short-Baseline Neutrino) program [73] at Fermilab exploits the Booster neutrino beam and 3 detectors: ICARUS, a 500 ton LAr TPC at a distance of 600 m, MicroBooNE which is located 470 meters away and has 80 tons of liquid argon, and Short-Baseline Near Detector, or SBND, at 110 meters with 112 tons fiducial mass. It aims at testing the sterile neutrino explanation for the LSND and MiniBooNE anomalies by looking for $\nu_\mu \rightarrow \nu_e$ oscillations at short distances. Thanks to the excellent detector capabilities, it has also a rich programme of exotic physics, e.g. heavy sterile neutrinos, dark matter searches. Experiments using reactor and radioactive source neutrinos with detectors at a distance of few meters from the source, such as DANSS, NEOS, SOLiD, PROSPECT, Neutrino-4, are ongoing and will be able to clarify the presence of a reactor neutrino anomaly by looking for electron antineutrino disappearance at different distances.

¹¹This explanation does not provide a particularly good fit to the MiniBooNE energy spectrum and alternative explanations for the latter have been put forward (see e.g. [69]).

3.4 Current knowledge of neutrino oscillation parameters and plans for the future

Thanks to the impressive programme discussed above, we have now a quite precise picture of neutrino properties, although some key questions remain unanswered.

The Δm_{21}^2 mass squared splitting is determined with very good accuracy to be $7.39 \times 10^{-5} \text{ eV}^2$ with a 3σ range of $6.79\text{--}8.01 \times 10^{-5} \text{ eV}^2$ [74]. The sign of this mass squared difference is positive. Δm_{31}^2 is known slightly less precisely and its sign is not yet established, leaving open two possibilities, normal (NO) or inverted (IO) ordering, see later. The measured values slightly differ between the orderings due to subleading effects in the oscillation probabilities. For NO one has $\Delta m_{31}^2 = 2.525$ ($2.431\text{--}2.622$) $\times 10^{-3} \text{ eV}^2$, for the best fit (3σ range) and similarly for IO $\Delta m_{32}^2 = -2.512$ ($-2.413\text{--}2.606$) $\times 10^{-3} \text{ eV}^2$ [74].

There are three mixing angles and they control the flavour content of the three mass eigenstates, given by $|U_{\alpha i}|^2$. Their values are known with quite good accuracy [74]:

$$\theta_{12} = 33.82 \text{ (31.61 – 36.27)} \quad \text{for both mass orderings,} \quad (39)$$

$$\theta_{23} = 49.7 \text{ (40.9 – 52.2) (NO)} \quad \theta_{23} = 49.7 \text{ (41.2 – 52.1) (IO),} \quad (40)$$

$$\theta_{13} = 8.61 \text{ (8.22 – 8.98) (NO)} \quad \theta_{13} = 8.65 \text{ (8.27 – 9.03) (IO),} \quad (41)$$

in degrees. We notice that all three angles are sizable and θ_{23} could even be maximal. The first hints of leptonic CPV have been reported, thanks to the combination of results from long-baseline experiments and of θ_{13} measurement by reactor neutrino experiments. Currently, there is a preference for large CP violation with $\delta = 217$ ($135\text{--}366$) (NO) and $\delta = 280$ ($196\text{--}351$) (IO), in degrees, although at 3σ the CP-conserving values $\delta = 0, 180^\circ$ for NO are still allowed. More data is required to confirm whether CP is violated in the lepton sector. No information on the Majorana phases is currently available. In Fig. 4 we report the two-dimensional projections in the neutrino mixing parameter space after marginalization with respect to the parameters not shown. The figure is taken from Ref. [74].

3.4.1 Future experiments

Future neutrino oscillation experiments aim at answering the questions related to the neutrino mass ordering, CP violation and the precise determination of the oscillation parameters, as well as providing important information on the Sun and supernovae. We provide here a concise review focusing on the main efforts currently planned.

DUNE. The DUNE experiment [75], exploiting the LBNF facility at Fermilab, will use a beam sourced at the Main Injector with 1.2 MW of power, upgraded to 2.4 MW after 6 years. The far detector will be constituted by 4 10 kton modules of LAr TPC, located at the Sanford Underground Research Facility site, at a distance of 1300 km from Fermilab. The first module is planned for 2024 and two technologies are being developed, the single phase and the dual phase LAr TPC ones. A near detector will be located at ~ 500 m from the target. Its design is being finalised. The flux has a broad spectrum with a peak around 3 GeV and a significant component at lower energies to optimise the sensitivity to CP violation. Thanks to the long baseline this experiment will see strong matter effects and will be able to determine the mass ordering at 5σ irrespective of the value of δ . The main drive for the experiment is the discovery of CP violation: DUNE will reach 3σ for 75% of the values of δ after an exposure of 1320 (850) kton MW years using the CDR (optimised) beam, and 5σ for 50% of the values of δ after 810 (550) kton MW years [75]. The LAr far detector is also an ideal target for SN neutrinos and will see atmospheric and solar neutrinos with a rich programme for non-accelerator neutrino physics and for proton decay.

Hyper-Kamiokande and T2HK long-baseline experiment. The Water-Cherenkov Hyper-Kamio-

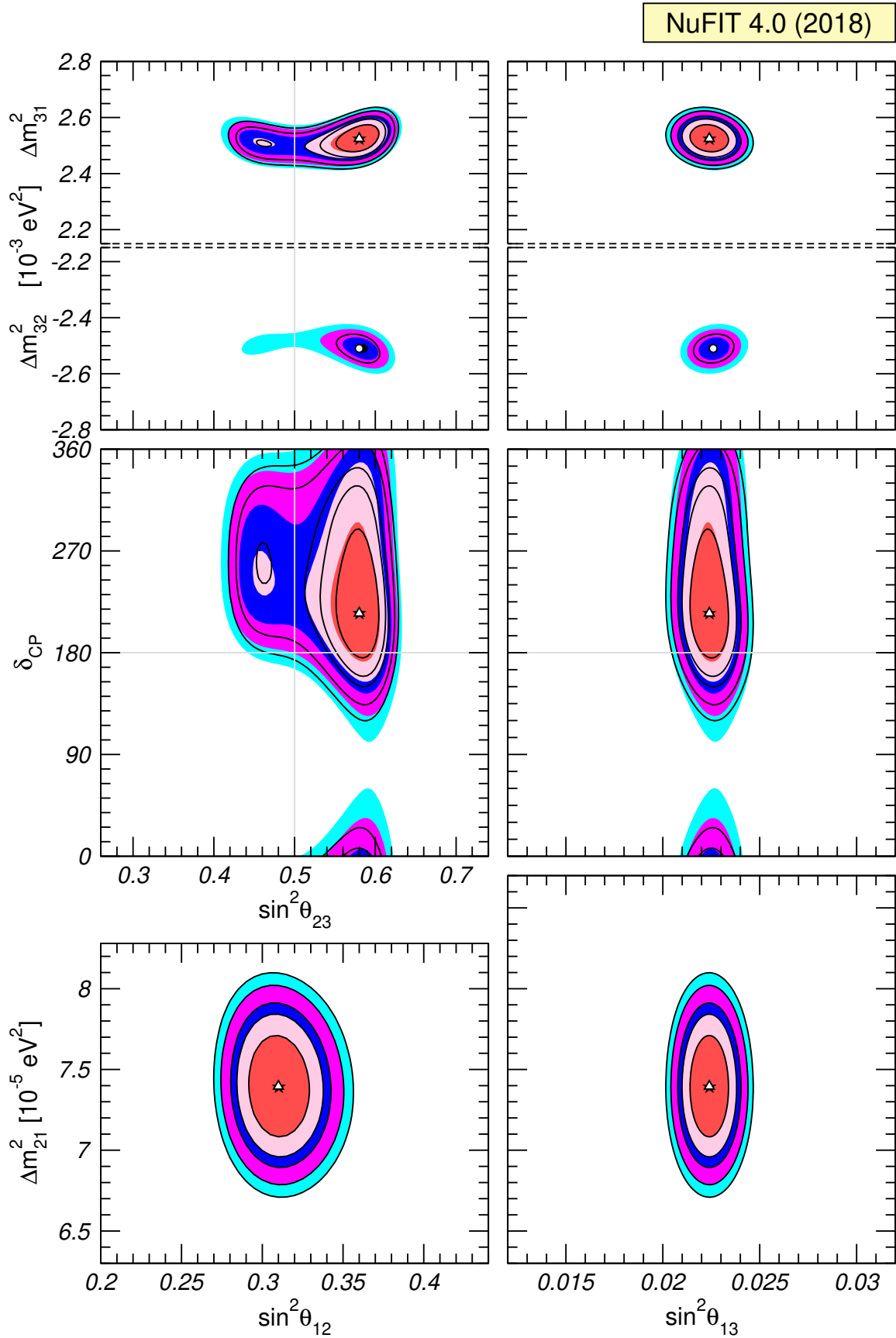


Fig. 4: Two-dimensional allowed regions in the neutrino parameters space at 1σ , 90%, 2σ , 99%, 3σ C.L.. The coloured regions (black contour curves) are obtained without (with) including the SK-atmospheric χ^2 data. Figure from Ref. [74].

kande detector [76] is the successor of Super-Kamiokande and will have a 187 kton fiducial mass per 1 tank, with improved detector capabilities. The optimal tank design will comprise two cylindrical detectors, 60 m in height and 74 m in diameter, with 40% photocoverage. Its main goals are the search for proton decay, the study of astrophysical neutrinos and to act as the target for a MW beam sourced at the J-PARC accelerator to discover CP violation. In regards to the beam, its location will be 2.5° off-axis at 295 km in the Tochibora mine. Its physics reach is due to excellent energy resolution for neutrino-nucleus quasi-elastic interactions, the large number of events and the low intrinsic background. With a total exposure of $1.3 \text{ MW} \times 10^8 \text{ s}$, it can establish leptonic CP violation at 3σ for 76% of the values of δ and discover it at 5σ for 58% of them, and will achieve an error on δ smaller than 22° for any value of δ ¹². The possibility to locate a second detector in South Korea is currently being investigated [77]. The longer baseline and higher energy, for a smaller off-axis angle, would allow to improve the sensitivity to the mass ordering as well as to CP violation and its precise determination.

Other accelerator neutrino experiments. ESS ν SB [78] would exploit a 10 MW beam, sourced at the European Spallation Source. For a far detector distance between 300 and 550 km, its spectrum is peaked around the second oscillation maximum in order to maximise the sensitivity to CP violation. With 500 kton Water-Cherenkov detector, this setup has the ability to discover CP violation at 5σ for up to 50% of the values of δ . Additional studies are currently ongoing in order to further optimise this facility. A neutrino factory [79] would constitute the ultimate neutrino oscillation experiment with unsurpassed physics reach. Neutrinos are produced by the decays of high energy muons in a decay ring, which source a collimated beam of muon neutrinos and electron antineutrinos. Magnetisation is necessary at the far detector to distinguish between muon neutrinos from the beam from muon antineutrinos from $\bar{\nu}_e \rightarrow \bar{\nu}_\mu$ oscillations. In the baseline design, a 100 kton magnetised iron MIND is used, 10 GeV muons and a source-detector distance of 2000 km. Thanks to the high number of events, very low backgrounds and the wide and well known energy spectrum, this setup would achieve a superior performance. For the sake of completeness, we mention that there are non-long-baseline strategies to search for leptonic CP violation. DAE δ ALUS (Decay-At-rest Experiment for δ_{CP} studies At the Laboratory for Underground Science) [80] uses a cyclotron-driven muon antineutrino beam aimed at a very large detector optimised for low energies at different distances in the few km range.

Atmospheric neutrinos. Very large detectors for atmospheric neutrinos are being planned or constructed and will have a very good sensitivity to the mass ordering and possibly to CP violation [81]¹³. Typically, these searches are performed as part of the high energy neutrino programme of IceCube2, KM3Net, in highly instrumented regions of the detector so that a lower energy threshold can be achieved. ORCA (Oscillation Research with Cosmics in the Abyss) [82] is part of KM3Net 2.0, with an intra-distance of 9 m between the digital optical modules, and could achieve a mass ordering discovery by 2024/25 if current hints of NO are confirmed. IceCube plans a near future upgrade with 7 additional strings in the Deep Core area, densely instrumented to study GeV neutrinos, and in a second phase IceCube Gen2 with a high-density core for low-energy neutrinos (PINGU) [83].

JUNO. The JUNO (Jiangmen Underground Neutrino Observatory) experiment [84], due to start data taking in 2021, will have a very rich experimental programme, both in astrophysical, terrestrial and reactor neutrinos. It will use a 20 kton LS (Liquid Scintillator) detector placed at a distance of 53 km from the 26.6 GW Yangjiang and Taishan Nuclear reactors and 700 m underground. It will have an unprecedented 3% energy resolution (at 1 MeV), necessary to study neutrino oscillations with great accuracy and in particular the interference between the solar and atmospheric amplitude contributions at $L/E \sim 10^4 \text{ km/GeV}$ [85, 86]. This effect is sensitive to the mass ordering and could lead to its discovery within few years in a way complementary to the exploitation of matter effects in accelerator and atmospheric neutrino experiments. Moreover, it will greatly increase the precision on the solar mixing

¹²The precision on δ is best for CP-conserving values while it is worse for maximal CPV, in vacuum.

¹³The latter aim is quite challenging and would require an effective volume of 5-10 Mton with an energy threshold of 0.5-1 GeV and excellent detector performance.

parameters with an expected 0.7% 1σ error on θ_{12} and 0.6% on Δm_{21}^2 . The accurate determination of θ_{12} is of great importance in distinguishing flavour models as it is a typical prediction for these models and enter sum-rules and other relations between the oscillation parameters. For instance, its value for tri-bimaximal mixing is $\sin^2 \theta_{12} = 1/3$, see Sec. 6.3.

Solar neutrinos. In addition to the dedicated Borexino experiment, several multipurpose detectors planned for the future will be able to provide information on solar neutrinos. Liquid scintillator detectors SNO+ and JUNO, LAr DUNE and Water-Cherenkov HK, as well as future ideas for water-based LSc Theia and the Jinping Slow LSc detector, could be used for this purpose with different energy thresholds, directionality and energy resolution capabilities. They will mainly focus on the regeneration of solar electron neutrinos while traversing the Earth, the so-called day/night effect, the precise shape of the probability from low energy to high energy, and, from the astrophysics point of view, getting information on the Sun. If their energy threshold and background reduction allow, they will also aim at the observation on the CNO and hep neutrinos.

4 Majorana and Dirac neutrinos

Neutral fermions could be either of Dirac or Majorana type, as first suggested by E. Majorana in 1937 [16]. In the first case, the particles and antiparticles are different as it is the case, e.g., for electrons and positrons. In the latter case, there is no distinction between particle and antiparticles. In the SM only neutrinos could be of Majorana type, as they are the only known neutral fermions. Their nature is strictly related to the conservation of lepton number and therefore offers an important window on the properties of the ultimate theory of particles. Processes which violate lepton number by two units can provide information on this important question, the most sensitive of which is neutrinoless double beta decay. A rich experimental programme is ongoing and planned for the future.

4.1 Charge conjugation

We start by defining the charge conjugate of a fermion field as

$$(\psi)^c(x) \equiv \xi_c C \bar{\psi}^T(x), \quad (42)$$

where ξ_c is the charge parity of the field. C is the charge conjugation matrix which satisfies the following properties

$$C \gamma_\mu^T C^{-1} = -\gamma_\mu, \quad (43)$$

$$C^\dagger = C^{-1}, \quad (44)$$

$$C^T = -C. \quad (45)$$

In the Dirac representation of the γ_μ matrices, one has $C = i\gamma^2\gamma^0$. Since two charge conjugation transformations must bring back the field to its initial value

$$\psi \xrightarrow{c} \xi_c C \bar{\psi}^T \xrightarrow{c} |\xi_c|^2 \psi, \quad (46)$$

we find $|\xi_c|^2 = 1$. The parameter ξ_c is a phase which represents the intrinsic charge parity of the field. From here onwards we take $\xi_c = 1$ for left-handed neutrinos¹⁴. Under a charge conjugation transformation, we have $\mathcal{U}_c \psi(x) \mathcal{U}_c^\dagger = \psi^c(x)$.

We notice an important property, that is, the charge conjugate of a left-handed field is right-handed and viceversa. In fact, using the left-handed projector P_L , one can show

$$P_L C \bar{\psi}_L^T = C (\bar{\psi}_L P_L)^T = C \left((P_R \psi_L)^\dagger \gamma^0 \right)^T = 0. \quad (47)$$

¹⁴Since weak interactions violate maximally the charge conjugation symmetry, the charge parity of neutrinos is arbitrary.

Under a charge conjugation transformation, we find that $\mathcal{U}_c \psi_L(x) \mathcal{U}_c^\dagger = (\psi_R(x))^c$. Therefore, a Lagrangian which contains only left-handed fields, such as the charge and neutral current terms in the Standard Model one, cannot preserve charge conjugation as a symmetry.

4.2 Majorana fields

A Majorana field is defined as

$$\psi = \psi^c . \quad (48)$$

This condition means that particle and antiparticle are indistinguishable and therefore can only apply to neutral fields. Majorana fields have several specific properties.

- Majorana fields satisfy the Dirac equation for particles and antiparticles

$$(i\gamma^\mu \partial_\mu - m)\psi = 0 . \quad (49)$$

- In terms of its chiral components the Majorana condition implies that the field can be written as

$$\psi = \psi_L + \psi_L^c , \quad (50)$$

where we have used the fact that $(\psi_L)^c = (\psi^c)_R$.

- Majorana fields have only 2 degrees of freedom, differently from Dirac ones which have 4.
- Majorana fields are quantised in terms of only one type of creation operator. The Fourier expansion is given by

$$\psi(x) = \int \frac{d^3p}{(2\pi)^3 \sqrt{2E}} \sum_{h=\pm 1} \left[a_h(p) u_h(p) e^{-ip \cdot x} + a_h^\dagger(p) v_h(p) e^{ip \cdot x} \right] , \quad (51)$$

where the Majorana condition has imposed $a_h = b_h$ compared to a Dirac field. So there is only one type of operator and there is no distinction between particle and antiparticle.

- Their electromagnetic current $j^\mu = q \bar{\psi} \gamma^\mu \psi$ vanishes exactly. Moreover, Majorana particles cannot carry any $U(1)$ quantum number.

In the SM only neutrinos are neutral fermions and can be Majorana particles. As they cannot carry any charge, this implies that lepton number is not a conserved symmetry if neutrinos are of Majorana type. This is evident from the fact that the Majorana condition is not invariant under a $U(1)_\mathcal{L}$ transformation and will become apparent considering Majorana mass terms. Therefore, the question of the nature of neutrinos is directly related to the fundamental symmetries of nature. Lepton number is an accidental symmetry of the SM, meaning that it is conserved at the Lagrangian level because of the gauge symmetry and particle content of the SM. Is the ultimate theory of particles lepton-number conserving or not? This question is intrinsically bound to neutrinos.

Commonly one still uses the notion of neutrino and antineutrino for Majorana fields, as far as neutrinos are ultrarelativistic (UR). An UR Majorana neutrino of negative helicity interacts as a Dirac neutrino with the same helicity and for this reason it is common to call this particle a neutrino. Conversely, an UR Majorana neutrino of positive helicity will behave as a Dirac antineutrino of the same helicity and will be called an antineutrino. We also stress that from the kinematic point of view Dirac and Majorana neutrinos are equivalent as they satisfy the same energy-momentum dispersion relation $E = \sqrt{\mathbf{p}^2 + m^2}$.

4.3 Neutrinoless double beta decay

Neutrino oscillations do not distinguish between Majorana and Dirac particles, as they conserve lepton number. To test this symmetry and establish the nature of neutrinos, it is necessary to search for processes which break lepton number. The most sensitive of these is neutrinoless double beta decay (DBD0 ν).

This process takes place in nuclei when two neutrons simultaneously decay into two protons and two electrons, with no neutrino emission. Its SM counterpart is the two-neutrino double beta decay (DBD 2ν), first proposed by M. Goeppert-Mayer in 1935 [87], in which two electron antineutrinos are produced:

$$\mathcal{N}(A, Z) \rightarrow \mathcal{N}(A, Z + 2) + 2e^- + 2\bar{\nu}_e \quad \text{for DBD}2\nu, \quad (52)$$

$$\mathcal{N}(A, Z) \rightarrow \mathcal{N}(A, Z + 2) + 2e^- \quad \text{for DBD}0\nu. \quad (53)$$

In 1939, W. H. Furry [88] proposed that this process could proceed without emission of neutrinos, if the latter are Majorana particles. Differently from DBD 2ν , neutrinoless double beta decay violates lepton number by two units and is not allowed by the SM. For this reason, its discovery would be of paramount importance and would imply that neutrinos are of Majorana type.

We restrict the discussion to the simplest and most studied case in which we add to the SM massive neutrinos, as required by the oscillation data. We assume that neutrinos are Majorana particles. The inverse of the half-life is given by

$$T_{\beta\beta 0\nu}^{-1} \simeq \frac{G_{0\nu}}{m_e} |m_{\beta\beta}|^2 M_{\text{NUCL}}^2, \quad (54)$$

where $G_{0\nu}$ is a known phase-space factor, m_e is the electron mass, M_{NUCL} is the nuclear matrix element for the nucleus of the process (NME). $m_{\beta\beta} \equiv m_{ee} \equiv \langle m \rangle$ is the *effective Majorana mass parameter* which embeds all the dependence on neutrino quantities as

$$|m_{\beta\beta}| \equiv \left| m_1 |U_{e1}|^2 + m_2 |U_{e2}|^2 e^{i\alpha_{21}} + m_3 |U_{e3}|^2 e^{i(\alpha_{31}-2\delta)} \right|. \quad (55)$$

Here, m_i , $i = 1, 2, 3$, indicate the three light neutrino masses, and U_{ei} are the elements of the first row of the PMNS lepton mixing matrix.

4.3.1 Predictions for the effective Majorana mass parameter

From Eq. (55) we see that the predicted value of $|m_{\beta\beta}|$ depends critically on the neutrino mass spectrum and on the values of the two Majorana phases in the PMNS matrix, α_{21} and α_{31} (see, e.g. Refs. [89, 90] and also Ref. [91]). We can consider the three limiting neutrino mass spectra discussed in Sec. 5, and we find that

$$|m_{\beta\beta}|^{\text{NH}} \simeq \left| \sqrt{\Delta m_{21}^2} \sin^2 \theta_{12} \cos^2 \theta_{13} + \sqrt{\Delta m_{31}^2} \sin^2 \theta_{13} e^{i(\alpha_{32}-2\delta)} \right|, \quad (56)$$

$$|m_{\beta\beta}|^{\text{IH}} \simeq \sqrt{|\Delta m_{32}^2|} \cos^2 \theta_{13} \sqrt{1 - \sin^2 2\theta_{12} \sin^2 \left(\frac{\alpha_{21}}{2} \right)}, \quad (57)$$

$$|m_{\beta\beta}|^{\text{QD}} \simeq m_0 \left| (\cos^2 \theta_{12} + \sin^2 \theta_{12} e^{i\alpha_{21}}) \cos^2 \theta_{13} + e^{i(\alpha_{31}-2\delta)} \sin^2 \theta_{13} \right|. \quad (58)$$

We can obtain the predictions for $|m_{\beta\beta}|$ and consequently the decay rates, by assuming a specific mass spectrum, substituting the measured values for Δm_{21}^2 , Δm_{31}^2 , θ_{12} , θ_{13} , and varying the CPV phases in their allowed ranges. We get, including a 3σ error on the oscillation parameters,

$$|m_{\beta\beta}|^{\text{NH}} \simeq 1.1 - 4.2 \text{ meV} \quad (59)$$

$$|m_{\beta\beta}|^{\text{IH}} \simeq 15 - 50 \text{ meV} \quad (60)$$

$$|m_{\beta\beta}|^{\text{QD}} \simeq (0.29 - 1)m_0. \quad (61)$$

In the most general case, varying the minimal value of neutrino masses, we show in Fig. 5 the current predictions for $|m_{\beta\beta}|$ for the two mass orderings.

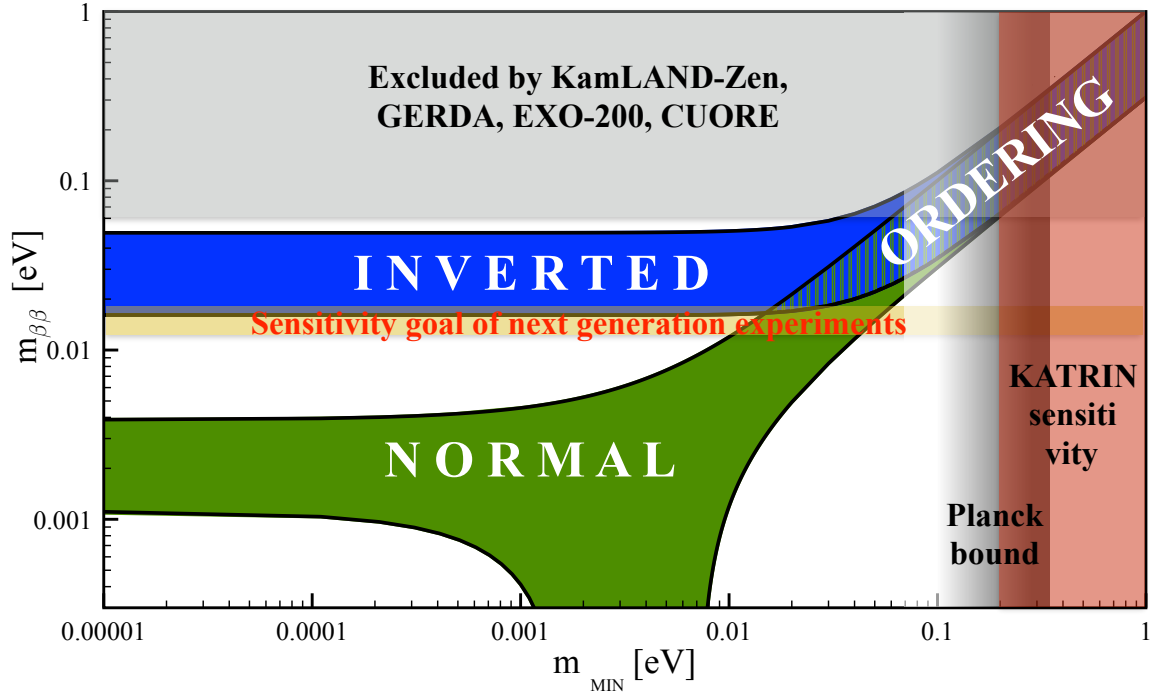


Fig. 5: The effective Majorana mass $|m_{\beta\beta}|$ at 2σ as a function of the smallest neutrino mass m_{MIN} . The Majorana phases α_{21} and α_{31} , and δ , are varied within their allowed intervals $[0, 180^\circ]$.

As it was noticed in Ref. [89] (see also Refs. [90]), in the case of *large but non-maximal solar mixing angle*, there is significant lower bound on $|m_{\beta\beta}|$ for IO given by

$$|m_{\beta\beta}|^{\text{IO}} \geq \sqrt{|\Delta m_{32}^2|} \cos 2\theta_{12} \simeq 15 \text{ meV} . \quad (62)$$

In the case of NO the effective Majorana mass can be zero even if neutrinos are Majorana particles due a cancellation for values of $m_{\text{MIN}} \sim 0.005 \text{ eV}$, as shown in Fig. 5.

It follows that neutrinoless double beta decay can provide information on the neutrino mass spectrum [89, 92, 93]. In the ideal case of perfectly known NME, a measurement of $|m_{\beta\beta}| > 0.1 \text{ eV}$ would imply that the spectrum is QD. For values of $|m_{\beta\beta}| < 15 \text{ meV}$ the ordering would necessarily be normal if neutrinos are Majorana particles. For values in between, both orderings are possible, but with constraints on the masses. For instance, for $15 \text{ meV} \leq |m_{\beta\beta}| \leq 50 \text{ meV}$, the neutrino mass spectrum could be inverted hierarchical or with NO and partial hierarchy with $m_1 > 15 \text{ meV}$. Similar, although somewhat weaker, conclusions can be obtained once the uncertainties on the NME and the experimental error on $|m_{\beta\beta}|$ are taken into account.

In principle, neutrinoless double beta decay could also tell us something about CP violation due to Majorana phases [89, 92, 94]. A very precise measurement of $|m_{\beta\beta}|$ and an accurate determination of the neutrino masses would open this possibility. However, this search is extremely challenging as it would require to know the NME with a very small error, at most at the few 10% level, which at present seems difficult to achieve.

4.3.2 Experimental status

Searches for 2-neutrino double beta decay started in the 40s and in 1950 the double beta decay half-life of ^{130}Te was measured with geochemical methods [95]. The first observation in a laboratory experiment

was carried out in 1987 using ^{82}Se [96]. Since then it has been observed in many other nuclei while neutrinoless DBD remains elusive. Double beta decay can be searched for in nuclei for which single beta decay is not kinematically allowed. These include e.g. ^{48}Ca , ^{76}Ge , ^{82}Se , ^{100}Mo , ^{130}Te , ^{136}Xe . In most experiments, the observation of double beta decay relies on the observation of the energy of the two electrons emitted. For neutrinoless double beta decay, the energy sits at the end point of the 2-electron spectrum as there is no neutrino emission and therefore the electrons carry away all the energy available. For DBD 2ν this is not the case and the spectrum is continuum reaching the end point. It follows that DBD 2ν is a background for DBD 0ν searches and excellent energy resolution is required to distinguish between the two¹⁵. These experiments are very challenging as they also require very low backgrounds, hence they are located deep underground and use ultra-pure components, and need large masses because of the very slow decay rate. After several years of development and construction, a new generation of experiments has recently started and is giving new results.

We provide a concise summary of the current bounds and the future prospects. Current limits on $m_{\beta\beta}$ correspond to the quasi-degenerate neutrino mass spectrum or with partial hierarchy for either ordering. The goal of the next generation of experiments is to test the values of $m_{\beta\beta}$ predicted for the inverted ordering and initial plans to go beyond are being discussed.

- Loaded liquid scintillator detectors. KamLAND-Zen uses ^{136}Xe which has the advantage of being available in large quantities. With an exposure of 126 kg yrs, KamLAND-Zen provides the current best bound on neutrinoless double beta decay: $T_{\beta\beta 0\nu} > 1.07 \times 10^{26}$ yrs and $|m_{\beta\beta}| < 61 - 165$ meV at 90% C.L. [97]. The detector mass is being increased to 750 kg of Xe in KamLAND-Zen 800 and subsequently there are plans to bring it to 1 ton in KamLAND2-Zen which, with an improved energy resolution, aims at $|m_{\beta\beta}| \sim 20$ meV close to the lower value predicted for inverted ordering. The SNO+ experiment is a multi-purpose detector using liquid scintillator and ^{130}Te to target $T_{\beta\beta 0\nu} > 10^{27}$ yrs [98]. It has not yet started data taking in this configuration. The possibility to use water-based scintillators might open the option of going to much bigger scales, such as in the 50 kton THEIA proposal, which with a 3% natural Te could reach $T_{\beta\beta 0\nu} > 10^{28}$ yrs and go as low as 5 meV in the effective Majorana mass parameter.
- Xe-based TPCs. EXO-200, with 110 kg active mass, has reached a bound of $T_{\beta\beta 0\nu} > 1.8 \times 10^{25}$ yrs and $|m_{\beta\beta}| < 147 - 398$ meV at 90% C.L. [99]. Plans for nEXO with 5 tons of Xe are being considered with a reach of $T_{\beta\beta 0\nu} > 9.2 \times 10^{27}$ yrs going below 10 meV for $|m_{\beta\beta}|$ in ten years [100]. NEXT [101] uses high pressure enriched Xe TPC and will reach $\sim 10^{26}$ yrs in a first phase and 1.5×10^{27} yrs in a second phase for the decay lifetime. The possibility to reduce the DBD 2ν backgrounds by tagging the daughter particle Ba^{++} seems promising. A similar effort is currently ongoing in China with the PANDAX-III experiment which ultimately aims at reaching the 1 ton scale [102].
- Germanium diodes. GERDA [103] uses high-purity Ge detectors, exploiting the decay of ^{76}Ge . This type of detectors have excellent energy resolution with no intrinsic backgrounds. Combining all results, for a total of 35 kg, a limit on $T_{\beta\beta 0\nu} > 0.8 \times 10^{26}$ yrs at 90% C.L. has been obtained. Weaker bound has been found by the Majorana collaboration, $T_{\beta\beta 0\nu} > 2.7 \times 10^{25}$ yrs at 90% C.L. [104]. Majorana and GERDA have combined their plans for the future in the LEG-END detector which aims at reaching the 10^{28} yrs sensitivity, corresponding to $|m_{\beta\beta}| < 11 - 23$ meV [105].
- Bolometers. CUORE searches for neutrinoless double beta decay in ^{130}Te using tellurium oxide bolometers. Combining the data from its demonstrator, CUORE-0, and Cuoricino, a bound of $T_{\beta\beta 0\nu} > 1.5 \times 10^{25}$ yrs at 90% C.L., corresponding to $|m_{\beta\beta}| < 110 - 520$ meV has been obtained [106]. There are plans to increase the mass and use ^{100}Mo in Li_2MoO_4 crystals to reach

¹⁵Ideas about the identification of the daughter nuclei, specifically in Xe, have been put forward and might become feasible in the future.

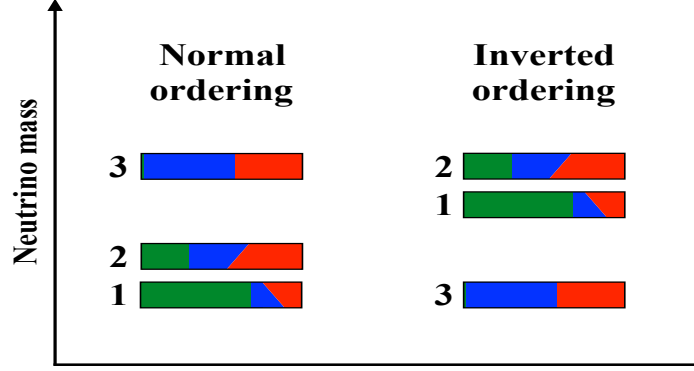


Fig. 6: Fractional flavour content, $|U_{\alpha i}|^2$ ($\alpha = e, \mu, \tau$), of the three mass eigenstates ν_i , based on the current best-fit values of the mixing angles. δ is varied from 0 (bottom of each coloured band) to 180° (top of coloured band), for normal and inverted mass ordering on the left and right, respectively. The different colours correspond to the ν_e fraction (green), ν_μ (blue) and ν_τ (red).

$T_{\beta\beta_{0\nu}} > 2.1 \times 10^{27}$ yrs, and $|m_{\beta\beta}| < 6 - 17$ meV. This effort called CUPID [107] will exploit scintillator bolometers to reduce backgrounds.

- Other efforts. The SuperNEMO experiment exploits a unique approach to track the individual electrons emitted in the decay. It uses a thin foil of $\beta\beta$ emitter surrounded by a low-density tracker and a fast calorimeter. In this way it can provide a full reconstruction of the event topology which could provide important information in terms of angular distribution, in case of a positive signal. The first demonstrator will start taking data this year using ^{82}Se . The COBRA (Cadmium-zinc-telluride 0-neutrino double Beta Research Apparatus) experiment uses the semiconductor CdZnTe detector technology that contains nine double beta decay isotopes: five decays $\beta^-\beta^-$ and four $\beta^+\beta^+$.

It should be noted that the extraction of $|m_{\beta\beta}|$ from a limit or future measurement on $T_{\beta\beta_{0\nu}}$ is affected by the theoretical evaluation of the NME. At present there are still large uncertainties in their computation and a strong theoretical effort is needed. Limits on $|m_{\beta\beta}|$ are given as a range which accounts for the uncertainty on the NME in the literature for a given nucleus.

5 Neutrino properties and open questions

The information on the mass squared differences from neutrino oscillation experiments indicates that there are three massive neutrinos and that we can order them in two ways¹⁶:

- normal ordering (NO): $m_1 < m_2 < m_3$, i.e. $\Delta m_{31}^2 > 0$,
- inverted ordering (IO): $m_3 < m_1 < m_2$, i.e. $\Delta m_{32}^2 < 0$.

In Fig. 6 we show the flavour content of each massive neutrino ν_i corresponding to $|U_{\alpha i}|^2$.

For each ordering¹⁷ the three neutrino masses can be expressed in term of just one unknown parameter, the lightest neutrino mass, m_{MIN} , see Fig. 7. We have

$$m_1 = m_{\text{MIN}}, \quad m_2 = \sqrt{m_{\text{MIN}}^2 + \Delta m_{21}^2}, \quad m_3 = \sqrt{m_{\text{MIN}}^2 + \Delta m_{31}^2}, \quad \text{for NO}; \quad (63)$$

¹⁶The convention of ordering the masses depends on the definition of the mixing angles, e.g. the correspondence between the solar mixing angle and θ_{12} . We adopt here the most widely used convention for which the meaning of the mixing angles does not change between the NO and IO.

¹⁷We prefer the use of “ordering” rather than hierarchy for neutrino masses, as it has not yet been established that they are indeed hierarchical.

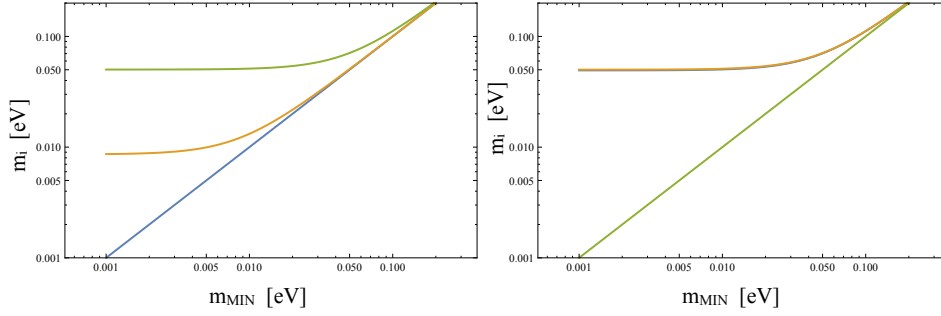


Fig. 7: Values of neutrino masses m_i (m_1 in blue, m_2 in orange and m_3 in green) for normal ordering (left) and inverted ordering (right) as a function of m_{MIN} . The current best-fit values of the mass squared-differences have been used [74].

$$m_3 = m_{\text{MIN}}, \quad m_1 = \sqrt{m_{\text{MIN}}^2 + |\Delta m_{32}^2| - \Delta m_{21}^2}, \quad m_2 = \sqrt{m_{\text{MIN}}^2 + |\Delta m_{32}^2|}, \quad \text{for IO.} \quad (64)$$

Therefore, determining the value of neutrino masses requires to establish the neutrino mass ordering and the absolute mass scale. Three different limiting cases can be identified:

- *Normal Hierarchical Spectrum (NH)*. For $m_{\text{MIN}} \rightarrow 0$, for NO we have $m_1 \ll m_2 \ll m_3$, with $m_1 \equiv m_{\text{MIN}}$, $m_2 \cong \sqrt{\Delta m_{21}^2}$ and $m_3 \cong \sqrt{\Delta m_{31}^2}$.
- *Inverted Hierarchical Spectrum (IH)*. In the limit $m_{\text{MIN}} \rightarrow 0$, for IO we have $m_3 \ll m_1 < m_2$, with $m_{1,2} \cong \sqrt{|\Delta m_{32}^2|}$ and $m_3 \equiv m_{\text{MIN}}$.
- *Quasi-Degenerate Spectrum (QD)*. For large values of m_{MIN} ($m_{\text{MIN}} \gg \sqrt{|\Delta m_{31}^2|}$) the three mass eigenstates are almost degenerate, $m_i^2 \simeq m_{\text{MIN}}^2 \equiv m_0^2$, $i = 1, 2, 3$.

On the mixing, it is interesting to note that leptonic mixing shows a very different pattern compared to quark mixing, which is rather small. In the leptonic mixing matrix, indeed two angles are very large, with θ_{23} which could be even maximal and θ_{12} which instead is far from maximality. The third mixing angle is significantly different from zero opening the possibility to search for matter effects and leptonic CP violation. The latter is one of the key open questions in this field as, in some models, it can be related to the baryon asymmetry of the Universe, see Sec. 6.4. The precise measurement of the oscillation parameters, including δ , is critical to hunt for the origin of the mixing structure and solve the leptonic flavour problem.

We note that we restrict our discussion to the 3-neutrino mixing scenario. As discussed earlier, controversial hints in favour of deviations from it, in terms of sterile neutrinos possibly with non-standard properties, have been found by experiments. A consistent picture has not emerged and tension is present with disappearance experiments and cosmology. Upcoming data will shed further light on these issues and we do not discuss them further.

5.1 Open questions regarding neutrino properties

The key open questions in current neutrino phenomenology can be summarised as follows:

- What is the nature of neutrinos? Are neutrinos Dirac or Majorana particles?
- What are the absolute values of the masses? In order to answer this question is necessary to establish the mass ordering and the overall mass scale.
- Is there leptonic CP violation? And if so, what is the precise value of the δ phase?
- What are the precise values of the mixing angles? Do they point towards an underlying flavour principle?

- Is the standard 3-neutrino picture correct or are there other effects, such as sterile neutrinos, non-standard interactions or even more exotic ones, e.g. Lorentz-violation?

We discussed in some detail the searches for neutrinoless double beta decay which can answer the first question. As discussed previously, the neutrino mass ordering can be determined in accelerator neutrino experiments, as well as atmospheric ones, exploiting matter effects, and in JUNO. Neutrinoless double beta decay can provide information on the neutrino mass spectrum as well, if neutrinos are Majorana particles. Cosmology can test the sum of neutrino masses, see Sec. 7.3. Direct neutrino mass searches aim at measuring the neutrino masses in a model independent way. They exploit the fact that in a beta decay the electron spectrum is affected by neutrino masses around the end point, as suggested initially by Fermi [108] and Perrin [109]. More specifically, for the values of the masses to which current experiments are sensitive, that is in the QD spectrum, the differential decay rate can be expressed as

$$\frac{d\Gamma_e}{dE_e} = \frac{G_F^2}{2\pi^3} m_e^5 \cos^2 \theta_C p_e (E_e + m_e) (E_0 - E_e) \sqrt{(E_0 - E)^2 - m_0^2} F(E_e) |\text{NME}_\beta|^2, \quad (65)$$

where E_e , p_e and m_e are the electron kinetic energy, momentum and mass, respectively. θ_C is the Cabibbo angle, $F(E_e)$ is the Fermi function arising from the Coulomb interactions of the final particles, NME_β is the nuclear matrix element. The nucleus of choice is currently tritium as it has several advantages. Its decay is superallowed so that the nuclear matrix element is constant and the beta spectrum is uniquely determined by phase space. The energy release Q is small, $Q = 18.6$ keV, which is beneficial since the high end part of the spectrum scales as Q^{-3} . The lifetime is not too long, $T_{1/2} = 12.3$ yrs. After the Troitzk and Mainz experiments set bounds in the eV range, $m_0 < 2.2$ eV [40], a new experimental effort using tritium is ongoing, the KATRIN project [110]. It will reach a sensitivity of 0.2 eV after three years of beam time. Ideas about using Cyclotron Radiation Emission Spectroscopy with atomic tritium are being explored by the Project 8 collaboration, with the ultimate goal of 0.04 eV. Other efforts, ECHO and HOLMES, exploit ^{163}Ho and, although are not currently competitive with KATRIN, will aim at obtaining sub-eV sensitivities in the future.

The hunt for leptonic CP violation is ongoing in long baseline neutrino oscillation experiments by observing the $\nu_\mu \rightarrow \nu_e$ transition channel. As discussed, first hints have been reported by T2K and NOvA in combination with Daya Bay and future experiments, in particular DUNE and T2HK, will be able to discover it for a large fraction of the parameter space. The same experiments can also provide a precise determination of the mixing angle θ_{23} , while JUNO will give the most accurate measurement of θ_{12} . Although accessible in principle in neutrinoless double beta decay experiments, it will be difficult to obtain information on Majorana CPV in the near future.

Regarding the last question, we just mention that there are several searches for sterile neutrinos both in neutrino oscillation experiments, e.g. the SBN programme at Fermilab and many reactor and radioactive source experiments, as well as in beta decay and other experiments. Present and future oscillation experiments can also search for non-standard neutrino properties and new interactions. The hunt is on.

5.2 Complementarity and synergy between different experiments

With the vast experimental programme currently ongoing or planned for the future, a strong complementarity and synergy between different strategies is present. We mention here some relevant examples.

- The determination of the mass ordering can be achieved exploiting matter effects in long baseline neutrino oscillation experiments in a very controlled manner in DUNE, as well as in atmospheric neutrinos and by looking for the $\Delta m_{21}^2 - \Delta m_{31}^2$ interference in reactor neutrino oscillations in vacuum. Given the importance of this issue, it is critical to have multiple experiments establishing the ordering. Once this is achieved, subdominant effects can be studied e.g. in atmospheric neutrinos

and important information can be deduced on supernovae (SN) evolution, once SN neutrinos are detected.

- Neutrinoless double beta decay and neutrino oscillation experiments. As shown in Sec. 4.3.1, the predictions for $|m_{\beta\beta}|$ depend on the neutrino mass ordering. If neutrino oscillation experiments determine that the neutrino mass ordering is inverted, $|m_{\beta\beta}|$ is predicted to be bigger than 15 meV providing a clear target for the neutrinoless double beta decay experiments. Further conclusions could be obtained depending on the experimental results. Let's first assume that the ordering is established to be inverted. (i) If $|m_{\beta\beta}| \geq 15$ meV, one can conclude that neutrinos are Majorana particles. Moreover, if $|m_{\beta\beta}| > 50$ meV both upper and lower bounds on m_3 can be deduced, given approximately by $|m_{\beta\beta}| \leq m_3 \leq |m_{\beta\beta}|/\cos 2\theta_{12}$. Consequently, a predicted range for the sum of neutrino masses relevant in cosmology could be found. For $15 \text{ meV} \leq |m_{\beta\beta}| \leq 50 \text{ meV}$, the spectrum would need to be inverted hierarchical. In principle, if a precise measurement of the masses is obtained from cosmological observations, CPV due to Majorana phases could be hunted for but a very precise determination of $|m_{\beta\beta}|$ would be needed. (ii) If $|m_{\beta\beta}| < 15$ meV is measured, neutrinos are also established to be Majorana particles but there must be some cancellation between the standard light neutrino mass contribution and new physics. The simplest example is the case of a light see-saw mechanism in which some of the heavy neutrinos have masses below 100 MeV. (iii) If only an upper bound below 15 meV is found on $|m_{\beta\beta}|$, then the simplest conclusion would be that neutrinos are Dirac particles, although a cancellation between the three-neutrino contribution and new physics could still be at work, for instance in the case of a light see-saw. It would be of particular importance to test this second hypothesis by looking for new particles and interactions which can give a sizable contribution to neutrinoless double beta decay. Let's now consider the case in which neutrino oscillation experiments determine that the ordering is normal, as first hints seem to indicate. We have seen that the predictions for $|m_{\beta\beta}|$ go from current bounds to a complete cancellation (see Fig. 5). A measurement of $|m_{\beta\beta}|$ would establish that neutrinos are Majorana particles and would restrict their masses to a specific range. We consider values up to few meV which may be at reach in a next-to-next generation of experiments. (i) If $|m_{\beta\beta}| \gg 4$ meV, the neutrino mass spectrum has a partial hierarchy, with $|m_{\beta\beta}| \leq m_1 \leq |m_{\beta\beta}|/\cos 2\theta_{12}$ with a predicted range for $\sum_i m_i$ in cosmology. (ii) If $|m_{\beta\beta}| \ll 4$ meV, and the process has not been observed, no conclusion can be drawn on the nature of neutrinos.
- Cosmology and terrestrial experiments. If terrestrial experiments establish that the ordering is inverted, $\sum_i m_i \geq 0.1$ eV. A precise measurement of its value would lead to an accurate determination of the values of neutrino masses, with implications for neutrinoless double beta decay as discussed above. If it is found that $\sum_i m_i < 0.1$ eV from cosmological observations, necessarily there are new cosmological or particle physics effects which reduce the impact of neutrino masses in the formation of large scale structures or which counter them.

6 Neutrino masses beyond the Standard Model

As we know that neutrinos have mass, it is necessary to augment the SM Lagrangian including the neutrino mass terms and then to explain the origin of these terms in a gauge invariant manner, hunting for the ultimate theory of particles and their interactions.

6.1 Dirac and Majorana mass terms

Being neutrinos Dirac or Majorana, different options are available to describe their masses.

- *Dirac masses.* The Lagrangian contains a mass term

$$-\mathcal{L}_{Dirac} = \bar{\nu} m_D \nu = \bar{\nu}_L m_D \nu_R + \text{h.c.} . \quad (66)$$

We notice that such mass term requires both ν_L and ν_R and is analogous to the mass terms for the SM charged fermions. This term conserves lepton number as it is possible to give both chiral components the same lepton number, so that under a $U(1)_{\mathcal{L}}$ transformation $\nu_{L,R} \rightarrow e^{i\eta}\nu_{L,R}$

$$\mathcal{L}_{Dirac} \xrightarrow{U(1)_{\mathcal{L}}} e^{i\eta} e^{-i\eta} \mathcal{L}_{Dirac} = \mathcal{L}_{Dirac} \quad (67)$$

the mass term remains invariant. Generically, there will be several neutrinos and the mass term contains a mass matrix M_D . In order to find the masses, it is necessary to diagonalise this mass matrix via a biunitary transformation $V_{\nu L}^\dagger M_D V_{\nu R} = \text{diag}(m_i)$: the eigenvalues correspond to the neutrino masses and the mass states are related to the initial states as $\nu_{iL} = V_{\nu L}^\dagger \nu_L$. The matrix $V_{\nu L}$ will then enter the CC Lagrangian, together with one coming from the diagonalisation of the charged lepton mass matrix, and from there neutrino oscillations.

- *Majorana masses.* Using only one Weyl spinor ν_L it is still possible to construct a mass term using the fact that $(\nu_L)^c$ is a right-handed field. It reads

$$-\mathcal{L}_{Majorana} = \frac{1}{2} \bar{\nu}^c m_M \nu = -\frac{1}{2} \nu_L^T C^\dagger m_M \nu_L + \text{h.c.} \quad (68)$$

This term is Lorentz invariant as both ν and ν^c behave in the same way under a Lorentz transformation. This term breaks lepton number by two units

$$\mathcal{L}_{Majorana} \xrightarrow{U(1)_{\mathcal{L}}} e^{2i\eta} \mathcal{L}_{Majorana} \quad (69)$$

For multiple ν_L , the mass m_M is promoted to a matrix M_M which needs to be diagonalised to find the values of the masses and the corresponding eigenstates. It can be shown that this matrix is symmetric, $M_M = M_M^T$, and can be diagonalised using one unitary matrix

$$V_\nu^T M_M V_\nu = m_{diag} \quad (70)$$

where m_{diag} contains the real and positive masses m_i . The massive fields $\nu_{i,L}$ will be related to the initial states ν_L as $\nu_{iL} = V_\nu^\dagger \nu_L$. If one defines the Majorana fields $\nu_i \equiv \nu_{i,L} + \nu_{i,L}^c$, this term can be rewritten as $-\mathcal{L}_{Majorana} = \frac{1}{2} m_i \bar{\nu}_i \nu_i$, showing that the resulting massive fields are of Majorana type.

- *Dirac plus Majorana masses.* In presence of both ν_L and ν_R fields, generically both Dirac and Majorana mass terms will be present

$$\mathcal{L}_{Dirac+Majorana} = -\bar{\nu}_L M_D \nu_R + \frac{1}{2} \nu_L^T C^\dagger M_{M,L} \nu_L + \frac{1}{2} \nu_R^T C^\dagger M_{M,R} \nu_R + \text{h.c.} \quad (71)$$

Defining the left-handed field

$$N_L \equiv \begin{pmatrix} \nu_L \\ \nu_R^c \end{pmatrix} \quad (72)$$

one can rewrite these Lagrangian terms as

$$\mathcal{L}_{Dirac+Majorana} = \frac{1}{2} N_L^T C^\dagger \mathcal{M} N_L + \text{h.c.} \quad (73)$$

where the mass matrix \mathcal{M} is given by

$$\mathcal{M} = \begin{pmatrix} M_{M,L} & M_D^* \\ M_D^\dagger & M_{M,R} \end{pmatrix} \quad (74)$$

Upon diagonalisation of this mass matrix, the mass eigenvalues can be found and the mass eigenstates $\nu_{i,L} = V_{D+M}^\dagger \begin{pmatrix} \nu_L \\ \nu_R^c \end{pmatrix}$. The resulting fields are Majorana, as expected since this Lagrangian breaks lepton number.

6.2 Neutrino masses beyond the SM

The mass terms discussed above are forbidden in the SM. There are no right-handed neutrinos and a Dirac mass term cannot be included. A Majorana mass term can be constructed using the ν_L fields only, but breaks the SM gauge invariance. Consequently, the SM, in its minimal form, does not allow for neutrino masses. In this sense, neutrino masses and mixing constitute the first particle physics evidence that the SM is incomplete. How can one extend it in order to account for neutrino masses in a consistent framework? A vast number of models has been proposed. We review here the key features of Dirac and Majorana mass models and we discuss more in detail the see-saw type I mechanism.

6.2.1 Dirac masses

The simplest extension which can be made to the SM involves adding new SM gauge singlets, called sterile neutrinos. We indicate them as ν_R . The following Yukawa coupling is allowed by the gauge symmetries

$$-\mathcal{L}_y = \bar{L}y_\nu \cdot \tilde{H}\nu_R + \text{h.c.} , \quad (75)$$

where $L \equiv (\nu_L^T, \ell^T)^T$ is the leptonic doublet, $\tilde{H} = i\sigma_2 H^*$ and H is the Higgs field. Once the neutral component of the Higgs field acquires a vacuum expectation value $\langle \tilde{H} \rangle = (v_H/\sqrt{2}, 0)^T$, this term generates a Dirac mass for the light neutrinos

$$-\mathcal{L}_y \xrightarrow{\langle \tilde{H} \rangle \neq 0} -\mathcal{L}_{Dirac} = \frac{v_H}{\sqrt{2}} \bar{\nu}_L y_\nu \nu_R + \text{h.c.} . \quad (76)$$

This Yukawa coupling and the resulting Dirac mass conserve lepton number. Indeed, as a Majorana mass term for ν_R is not forbidden by gauge invariance, its absence must be imposed by requiring lepton number conservation. In this case, this symmetry needs to be promoted from being an accidental symmetry of the SM to a fundamental ingredient of the theory of particle interactions. In this sense, this is a major departure from the Standard Model.

We can estimate the order of magnitude of the coupling y_ν . Working in a one generation case, taking $m_\nu = y_\nu v_H/\sqrt{2}$ to be sub-eV, we get that $y_\nu \sim 10^{-12}$. This is a very small number and in this minimal model there is no explanation for the very strong hierarchy of masses between the charged leptons and the neutrinos. Moreover, one would naively expect a similar hierarchy between the neutrino masses and a similar mixing structure to the quark sector, contradicting the observations. For these reasons, other explanations for neutrino masses have also been considered.

6.2.2 Majorana masses and the Weinberg operator

Among all SM fermions, neutrinos are the only ones that can have a Majorana mass term. Noticing that the term $\bar{L} \cdot \tilde{H}$ is gauge invariant, it is possible to construct a singlet combination [111]

$$\mathcal{L}_{M,BSM} = \frac{\lambda}{\Lambda} L^T \cdot \tilde{H}^* C^\dagger \tilde{H}^\dagger \cdot L + \text{h.c.} . \quad (77)$$

This term, called the Weinberg operator, has dimension 5 and requires a mass scale Λ in the denominator. It should be pointed out that this operator is the only $D = 5$ admitted by the SM, with other effective operators being of higher dimension. Its presence is of great importance. It suggests that there is a new theory at a high scale Λ which is integrated out at low energies. This is in analogy to the Fermi theory being the low energy realisation of the weak interactions mediated by the W boson. The hunt for the new particles and interactions involved is at the centre of much of current research in theoretical neutrino physics.

The Weinberg operator breaks lepton number by two units and leads to a Majorana mass term once the Higgs boson gets a vacuum expectation value

$$\mathcal{L}_{M,BSM} \xrightarrow{\langle \tilde{H} \rangle \neq 0} \frac{\lambda v_H^2}{2\Lambda} \nu_L^T C^\dagger \nu_L + \text{h.c.} . \quad (78)$$

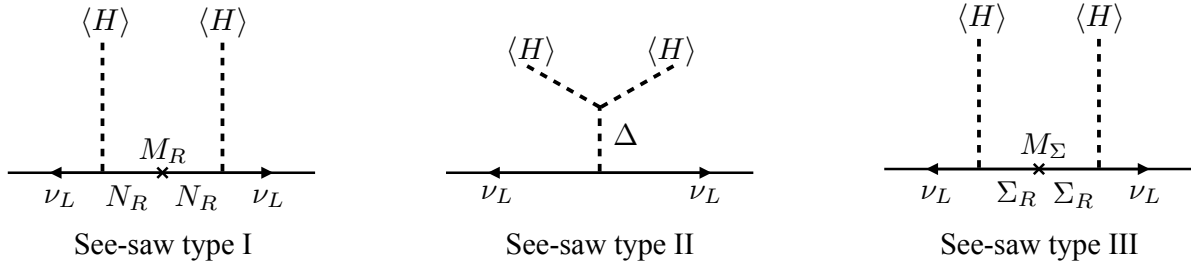


Fig. 8: Diagrams contributing to light neutrino masses in the three see-saw cases. $\langle H \rangle$ indicates the vev of the neutral component of the Higgs field. Δ is a scalar triplet and Σ is the neutral component of a fermion triplet, with mass M_Σ .

The resulting massive neutrinos are of Majorana type.

6.2.3 Hunting for the origin of the Weinberg operator: the seesaw mechanism

As the Weinberg operator is a low energy effective term, the key question revolves around the physics responsible for it. We can proceed by analogy with the Fermi theory. In the latter case, the four-fermion interaction is mediated at high energy by the exchange of a massive boson at tree level. For energies much smaller than the boson mass, its presence is felt in the m_W^2 term in the propagator, which enters G_F . Also in the case of the Weinberg operator one can consider the exchange of virtual massive particles at tree level. Their mass M corresponds to the scale Λ . There are three main options which have been classified based on the exchanged particle as

- see-saw type I [112] for a singlet fermion;
- see-saw type II [113] using heavy triplet scalars;
- see-saw type III [114] for triplet fermions.

In Fig. 8 we schematically show the contribution to neutrino masses in the three cases. In many extensions, the scale Λ is taken to be at or close to the Grand Unification one, $\sim 10^{14}$ GeV. The advantage of this formulation is that large couplings are allowed and the suppression of neutrino masses is due to the heavy masses. Moreover, see-saw mechanisms can be embedded in GUT theories, for instance see-saw type I naturally emerges in $SO(10)$ models. This choice remains very popular and has the added advantage that leptogenesis can be readily embedded in this framework providing an explanation for the baryon asymmetry of the Universe. The drawback is that it would be impossible to test such models, apart from a rather indirect indication coming from proton decay. Moreover, if a stabilising mechanism for the electroweak breaking scale, e.g. supersymmetry, is absent, the new physics will generically induce a correction to the Higgs mass and this suggests a scale lower than 10^7 GeV [115]. In order to lower the scale and make the models directly testable, one can consider smaller couplings. A lot of attention has been devoted to the TeV scale as this is accessible at the LHC. New particles, such as scalar and fermion triplets as well as sterile neutrinos would leave characteristic signatures. For instance sterile neutrinos would induce same-sign dileptons plus jets with no missing energy and lepton flavour violating signals [116, 117]. Searches of this kind have been made at LHCb [118], ATLAS [119], CMS [120], Belle [121]. Allowing for even smaller couplings would lower the scale further, with heavy neutrinos with GeV, MeV and even eV masses. These low energy see-saw models have very interesting signatures which depend on their mass and flavour mixing. For eV masses, they will induce neutrino oscillations at short distances. In the keV range, their emission in beta decays distorts the electron spectrum with kinks and for very small mixing angles they could be stable on cosmological timescales providing a candidate for dark matter [122]. For MeV-GeV masses they induce peaks in the spectrum of electrons and muons emitted in meson decays [123]. These so-called peak searches are rather model independent and

provide very strong constraints on the mixing angles [124, 125] with new results being recently provided by the NA62 experiment [126]. Another strategy to search for them is to look for their decays once they are produced in meson or lepton decays [127]. Past experiments such as PS191 [128] set some of the strongest bounds for 100s of MeV masses and present/future experiments used in beam dump mode, e.g. T2K [129], NA62, DUNE, T2HK, as well the purpose made SHiP one will be able to improve on current bounds [130]. It should be noted that these bounds could be significantly modified and weakened if additional interactions lead to fast invisible decays. If the heavy neutral leptons are Majorana particles they will induce lepton number violating processes, such as neutrinoless double beta decay and LNV meson and tau decays [117, 131]. The GeV mass range is of particular interest as these sterile neutrinos could be at the origin of the baryon asymmetry of the Universe via the ARS mechanism [132, 133].

Apart from making the couplings smaller and smaller, there are other ways to enhance the testability of neutrino mass models. Research has been done in models in which neutrino masses are forbidden at tree-level and arise at the loop one [134–136]. Another possibility is to extend the see-saw framework imposing a quasi-preserved lepton number symmetry. This is the case for inverse and linear, as well as extended, see-saws [137]. For instance in the inverse see-saw mechanism, one introduces multiple sterile neutrinos and imposes a quasi-preserved lepton number symmetry. The smallness of neutrino masses is explained in terms of small lepton number violating parameters and the heavy states are pseudo-Dirac¹⁸ particles which can have sizable mixing with the active neutrinos.

6.2.4 See-saw type I model

The see-saw type I mechanism is the simplest extension of the SM which can explain not only neutrino masses but also their smallness. It breaks lepton number by two units and predicts Majorana neutrinos.

Let's introduce 2 or more¹⁹ sterile neutrinos $N_{j,R}$, $j > 1$. These are fermions with no SM gauge numbers. The most general Lagrangian which respects the SM gauge group reads

$$\mathcal{L}_{\text{seesaw}} = \mathcal{L}_{\text{SM}} - \sum_{j,\alpha} \bar{L}_\alpha y_{\alpha j} \cdot \tilde{H} N_{j,R} + \sum_{j,k} \frac{1}{2} N_{j,R}^T C^\dagger M_{N,jk} N_{k,R} + \text{h.c.}, \quad (79)$$

where y is a $3 \times j$ matrix and M_N is a $j \times j$ symmetric Majorana mass matrix. Without loss of generality one can choose to work in the basis in which M_N is real and diagonal with heavy masses M_j . Once the neutral component of the Higgs boson gets a vev, the Yukawa term will induce a Dirac mass for the neutrinos $m_D \equiv y v_H / \sqrt{2}$. In the $\nu_{\alpha,L} - N_{j,R}$ basis the mass terms read

$$\mathcal{L}_{\text{seesaw,mass}} = \frac{1}{2} \left((\nu_L^c)^T \quad N_R^T \right) C^\dagger \begin{pmatrix} 0 & m_D \\ m_D^T & M_N \end{pmatrix} \begin{pmatrix} \nu_L^c \\ N_R \end{pmatrix} + \text{h.c.} \quad (80)$$

This Lagrangian is of the Dirac+Majorana form discussed in Eq. (74).

We consider the limit²⁰ in which $m_D \ll M_N$. Upon diagonalisation of the mass matrix, we find that the heavy neutrinos remain mainly in the sterile neutrino direction, hence their name of nearly-sterile neutrinos, and have mass $\sim M_j$. The light neutrinos, mainly in the active component, acquire a small mass

$$m_\nu \simeq -m_D \frac{1}{M_N} m_D^T. \quad (81)$$

The larger M_N the smaller the neutrino masses, hence the name of *see-saw*. The smallness of neutrino masses is due to the large hierarchy between the m_D and M_N scales. If we take M_N at the GUT scale and m_D of the same order of the charged fermions, one can easily obtain neutrino masses in the right

¹⁸Pseudo-Dirac particles are Majorana particles which have nearly degenerate masses with opposite CP-parity. If the masses were exactly equal, they would form a Dirac pair.

¹⁹At least two heavy neutrinos are required to reproduce two mass squared differences.

²⁰In the opposite case, $M \rightarrow 0$, we recover lepton number conservation and Dirac masses for the neutrinos.

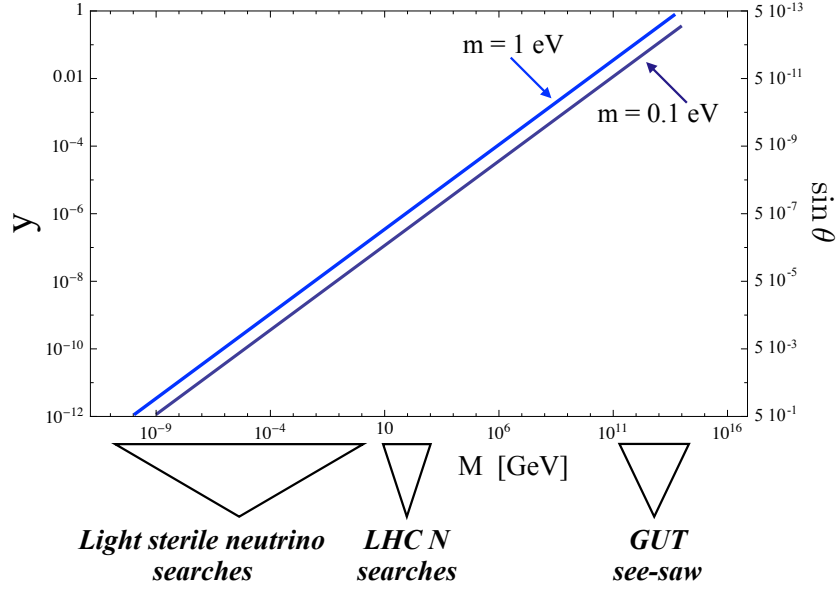


Fig. 9: Yukawa coupling versus nearly-sterile neutrino mass needed to generate a light neutrino mass $m = 1\text{--}0.1$ eV. The corresponding value of $\sin \theta$ is also indicated. Experimental strategies to search for the nearly-sterile neutrinos in the mass ranges of interest are schematically reported.

ballpark. In Fig. 9 we show the values of the Yukawa couplings required to give a light neutrino mass m_ν in a simplified one-generation case. The mixing angle between the heavy neutrino and the active one is $\sin^2 \theta = m_\nu/M_N$ and therefore typically very small.

It is useful to consider the number of free parameters. For 3 sterile neutrinos, a see-saw type I model has 3 heavy masses, 9 real parameters in the Yukawa coupling and 6 phases. Of these only 3 light neutrino masses, 3 mixing angles and 3 phases can be measured at low energy²¹. If the scale is sufficiently low, some additional parameters, e.g. the heavy neutrino masses, might be at reach. A useful parameterisation allows to separate the high energy parameters from the low energy observable ones. This is the so-called Casas-Ibarra parameterisation [138]

$$y = \frac{i\sqrt{2}}{v_H} V^* \text{diag}(m_\nu)^{1/2} R M_R^{1/2}, \quad (82)$$

where R is a complex orthogonal matrix so that $RR^T = 1$.

6.3 Leptonic mixing

Apart from neutrino masses, the other key question in neutrino theory is the origin of the observed leptonic flavour structure. It is significantly different from the one in the quark sector [40, 74], which is close to the identity with correction of order $\lambda \sim 0.2$ and its powers λ^2, λ^3 . We have for the U_{PMNS} and the CKM mixing matrices

$$|U_{\text{PMNS}}|_{3\sigma} = \begin{pmatrix} 0.797 - 0.842 & 0.518 - 0.585 & 0.143 - 0.156 \\ 0.233 - 0.495 & 0.448 - 0.679 & 0.639 - 0.783 \\ 0.287 - 0.532 & 0.486 - 0.706 & 0.604 - 0.754 \end{pmatrix}, \quad (83)$$

$$|V_{\text{CKM}}| = \begin{pmatrix} 0.97427(14) & 0.22536(61) & 0.00355(15) \\ 0.22522(61) & 0.97343(15) & 0.0414(12) \\ 0.00886(33) & 0.0405(12) & 0.99914(5) \end{pmatrix}. \quad (84)$$

²¹Realistically only one CPV phase can be measured in long baseline neutrino oscillation experiments and the determination of the two Majorana phases will remain most likely out of reach.

Motivated by the measured values of the mixing angles, in particular θ_{23} being (nearly) maximal and θ_{13} being smaller than the other two angles, a lot of attention has been devoted to leading-order patterns. They typically have $\sin^2 2\theta_{23} = 1$, $\sin^2 2\theta_{13} = 0$ and various values for θ_{12} . Among these, the most popular patterns include the tri-bimaximal (TBM) one [139], with $\sin^2 2\theta_{23} = 1$, $\sin^2 \theta_{12} = \frac{1}{3}$, $\sin^2 \theta_{13} = 0$ and the bimaximal (BM) one [140], with $\sin^2 2\theta_{23} = 1$, $\sin^2 2\theta_{12} = 1$, $\sin^2 \theta_{13} = 0$. Other cases are the golden ratio, trimaximal or hexagonal mixing, see e.g. Ref. [141], and it is also possible to have non-zero θ_{13} from the start. The basic idea is to invoke a principle, e.g. a flavour symmetry, which leads to such a pattern and then introduce corrections to reproduce $\sin \theta_{13} \neq 0$, if needed, and deviations from the canonical values of the angles. In order to achieve this goal a specific form of the neutrino and charged lepton mass matrices is imposed.

We recall that the neutrino mass matrix and its eigenvalues (i.e., the neutrino masses) are related by a unitary matrix V_ν ²² as

$$\text{diag}(m_1, m_2, m_3) = V_\nu^T \mathcal{M}_\nu V_\nu. \quad (85)$$

In a similar manner, the charged lepton mass matrix can be diagonalised using two unitary matrices V_ℓ and V'_ℓ , the first acting on the chiral fields ℓ_L and the latter on ℓ_R . The mass eigenstates, with definite non-negative masses, are what we commonly refer to as “electron”, “muon” and “tau” leptons, which are differentiated only by their masses. The PMNS mixing matrix, which enters the CC interactions and whose elements can be measured in neutrino oscillation experiments, emerges from the product of the two transformations

$$U_{\text{PMNS}} = V_\ell^\dagger V_\nu, \quad (86)$$

which inherits the flavour structure from both the neutrino and charged lepton sectors.

Various theoretical approaches have been invoked to explain the observed structure of the PMNS matrix. As the neutrino mixing angles do not exhibit a very strong hierarchy, the notion of anarchy [142] was put forward in which the values of all the entries of \mathcal{M}_ν are of the same order. Anarchy models can reproduce the observed values of the neutrino parameters but offer no further insight into the leptonic flavour problem.

An alternative approach is to invoke a guiding principle which dictates the values of the mixing angles, given the fact that θ_{23} is close to maximal and θ_{12} is not far from special numerical values such as $1/\sqrt{3}$. The most popular strategy is to employ flavour symmetries and control their breaking. Significant work has been done using non-abelian discrete groups S_4 , A_4 , A_5 , D_N , $\Sigma(2N^2)$, $\Sigma(3N^3)$, $\Delta(3N^2)$, $\Delta(6N^2)$ (for reviews see e.g. Refs. [143]) and the continuous groups $SU(3)$ [144] and $SO(3)$ [145]. The leptonic doublets are charged under a given flavour symmetry G_f which needs to be subsequently broken, as the charged lepton masses are non-degenerate [146]. The breaking needs to lead to different structures in the charged lepton and the neutrino sectors, typically Abelian residual symmetries G_ℓ and G_ν . These groups constrain the form of the neutrino and charged lepton mass matrices, leading to V_ℓ and V_ν and ultimately to U_{PMNS} .

We do not enter into a detailed discussion of leptonic flavour models as the literature is very vast. Instead, we give a simple illustration of how a symmetry can induce a specific value for a mixing angle. Let's assume a $L_\mu - L_\tau$ symmetry in a 2-neutrino mixing scenario. The neutrino mass matrix is forced to have the following structure:

$$\mathcal{M}_\nu = \begin{pmatrix} a & b \\ b & a \end{pmatrix}, \quad (87)$$

where we take a and b to be two arbitrary parameters which satisfy the hierarchy $a \ll b$. The diagonalisation of this matrix leads to two quasi-degenerate neutrino masses $b \pm a^{23}$ and to maximal mixing

²²We refer here to the neutrino mixing matrix as V_ν , in a generic basis for the charged leptons. Previously, we used the PMNS mixing matrix in the basis in which the charged leptons are in the mass eigenstate basis.

²³A negative sign for the neutrino mass can be absorbed into a redefinition of the neutrino field via its Majorana phase.

$\theta = 45^\circ$. A structure of this kind could be employed to explain a maximal atmospheric mixing angle and an inverted hierarchical spectrum. This reasoning can be extended to three-neutrino mixing.

It is very common for models based on flavour symmetries to have correlations between mixing parameters, usually the mixing angles and the CPV phases [147–149]. To start with, the leading-order mass matrices have very few parameters once the flavour symmetry is imposed. The corrections introduced to shift the angles also typically depend on very few quantities, leading to correlations between the mixing parameters commonly known as *sum rules*. They can be typically divided into two main classes:

- atmospheric sum rules [148], which are of the type $\sin^2 \theta_{23} = 1/2 + \zeta \sin \theta_{13} \cos \delta$, with ζ a real parameter predicted by the model. An important example is trimaximal mixing, which can be obtained from TBM pattern using a rotation in the 2-3 or 1-3 plane: $\sin^2 \theta_{23} = 1/2 - \sqrt{2} \sin \theta_{13} \cos \delta$ and $\sin^2 \theta_{23} = 1/2 + 1/\sqrt{2} \sin \theta_{13} \cos \delta$, respectively.
- solar sum rules [149–151] for which $\sin^2 \theta_{12} = 1/3 + \zeta' \sin^2 \theta_{13} \cos \delta$, with ζ' a real parameter given by the model. They often arise in models in which the leading-order mixing matrix receives corrections from the charged lepton sector. In models motivated by Grand Unified Theories (GUTs), the charged lepton mass matrix is related to the down-type quark one and V_ℓ gets corrections of the order of the Cabibbo angle.

It is interesting to note that, as the values of the mixing angles are known with good accuracy, the sum rules amount to predictions for the δ phase. For instance, focusing on solar sum rules, assuming that there are no 1-3 rotations in V_ν or V_ℓ at leading order, $\cos \delta$ is predicted to be [152]

$$\cos \delta = \frac{t_{23} \sin^2 \theta_{12} + \sin^2 \theta_{13} \cos^2 \theta_{12} / t_{23} - \sin^2 \theta_{12}^\nu (t_{23} + \sin^2 \theta_{13} / t_{23})}{\sin 2\theta_{12} \sin \theta_{13}}, \quad (88)$$

where $t_{23} \equiv \tan \theta_{23}$. θ_{12}^ν is the value in V_ν predicted by the flavour symmetry at leading order, e.g. $\sin^2 \theta_{12}^\nu = 1/3$ for TBM and $\sin^2 \theta_{12}^\nu = 1/2$ for BM. Present and/or future oscillation experiments can test these relations and provide useful insight on the origin of the observed leptonic flavour structure.

The possibility to impose a symmetry associated with CP at the Lagrangian level has also been investigated. It requires the introduction of a generalised CP symmetry [153–155] which is a combination of charge conjugation and parity and acts in a non-trivial manner on the flavour indices of a field ψ :

$$\psi(x) \rightarrow X\psi^c(x'). \quad (89)$$

Here, $x' = (t, -\mathbf{x})$ and X is a symmetric unitary matrix ($XX^* = X^*X = 1$) which guarantees that the original state is recovered after applying the transformation twice. The basic idea is to combine this symmetry with a discrete flavour one. Typically, definite predictions for the CPV phases, including the Majorana ones, emerge in this scheme, leading to testable signatures in neutrino oscillation and neutrinoless double beta decay experiments.

6.4 Leptogenesis and the baryon asymmetry

The origin of the matter-antimatter asymmetry in the Universe is one of the most compelling questions in cosmology. Its value has been well measured using the cosmic microwave background (CMB) radiation by Planck [156]

$$Y_B^{\text{CMB}} \simeq (8.67 \pm 0.09) \times 10^{-10}, \quad (90)$$

where Y_B is the baryon to photon ratio at recombination and is in good agreement with the one derived from Big Bang Nucleosynthesis (BBN).

Assuming that the Universe started with the same amount of baryons and antibaryons, as suggested by inflationary models, the baryon asymmetry can be dynamically generated if the Sakharov conditions [157] are satisfied:

- *Baryon number violation* (or Lepton number violation, for the leptogenesis mechanism). In the SM B and L are accidental symmetries which are conserved at the perturbative level. However, $B + L$ is anomalous and transitions which violate lepton and baryon number can happen at sufficiently high temperatures via thermal excitations with topological charge called sphalerons. This implies that a violation of lepton number can induce a baryon asymmetry.
- *C and CP violation*. If CP is conserved, every reaction which produces a particle will be accompanied by the opposite one creating an antiparticle, so that there is no net creation of a baryon number.
- *Departure from thermal equilibrium*. In equilibrium, the production and destruction of a baryon asymmetry proceed with the same rate. This condition is readily satisfied by the expansion of the Universe.

Several mechanisms have been proposed to explain the origin of the baryon asymmetry. Here we focus on one of the most popular and successful: leptogenesis [158]. The basic idea is that a lepton number is created in the Early Universe and this is then converted into a baryon number. This conversion happens in the SM itself at the non-perturbative level by sphaleron effects [159].

Leptogenesis is particularly appealing because it can naturally take place in see-saw models [112]. For simplicity, we focus only on leptogenesis in see-saw type I models, but it is possible to embed this mechanism also in other neutrino mass models. A see-saw type I model can satisfy the three Sakharov conditions: (i) lepton number is violated by the Majorana M_N term; (ii) CP violation can be present in the y matrix if it is complex; (iii) the departure from equilibrium is due to the N_j decays in the expanding Universe, once the temperature drops below their mass.

At very high temperatures, the heavy neutrinos N_j are in thermal equilibrium with the rest of the plasma thanks to their Yukawa interactions

$$N_j \leftrightarrow H^0 \nu_L, \quad N_j \leftrightarrow H^+ \ell. \quad (91)$$

As the Universe cools, T becomes smaller than M_j implying the particles in the plasma do not have sufficient energy to produce back right handed neutrinos. Only their decays are allowed

$$N_j \rightarrow H^0 \nu_L, \quad N_j \rightarrow H^+ \ell. \quad (92)$$

Being Majorana neutrinos, N_j can decay both into one channel and its charge conjugate one

$$N_j \rightarrow H^- \ell^+, \quad N_j \rightarrow H^+ \ell^-. \quad (93)$$

If the rates of these two processes are different, due to CP violation, then a net charge asymmetry ε is generated. This process is not instantaneous and washout effects, due e.g. by inverse decays, will partly erase the asymmetry. The remaining lepton asymmetry can then be converted by sphaleron processes into a baryon asymmetry. The latter depends on

$$\eta_B \propto k c_s \varepsilon_1, \quad (94)$$

where k is the washout factor which takes into account the fact that the decoupling is not instantaneous, c_s is the sphaleron constant which quantifies how much of the lepton asymmetry is converted to a baryon asymmetry, ε_1 is the CP-asymmetry given by $\varepsilon_1 \equiv \frac{\Gamma(N \rightarrow lH) - \Gamma(N \rightarrow l^c H^c)}{\Gamma(N \rightarrow lH) + \Gamma(N \rightarrow l^c H^c)}$.

At high temperatures, $T > 10^{12}$ GeV, different leptonic flavours cannot be distinguished as their Yukawa interactions are out of equilibrium. In this case, assuming $M_1 \ll M_2 \ll M_3$, it is useful to consider only the total CP-asymmetry [158, 160, 161] :

$$\varepsilon_1 = \frac{\Gamma(N_1 \rightarrow H^- \ell^+) - \Gamma(N_1 \rightarrow H^+ \ell^-)}{\Gamma(N_1 \rightarrow H^- \ell^+) + \Gamma(N_1 \rightarrow H^+ \ell^-)} \simeq \frac{3}{16\pi v_H^2} \sum_{j \neq 1} \frac{\Im(m_D m_D^\dagger)_{1j}^2}{(m_D m_D^\dagger)_{11}} \frac{M_1}{M_j}. \quad (95)$$

Once the interactions due to the charged lepton Yukawa couplings get into equilibrium, at $T \sim 10^{12}$ GeV for τ leptons and at $T \sim 10^9$ GeV for muons, different lepton flavours become distinguishable and the asymmetry and wash-out effects become flavour-dependent. The total lepton asymmetry can be obtained summing the separate contributions of each flavour CP asymmetry washed-out by the same-lepton number violating processes [162]. Each flavour asymmetry is given by

$$\varepsilon_l = \frac{3}{16\pi v_H^2} \frac{1}{(m_D m_D^\dagger)_{11}} \Im \left(\sum_j \left((m_D)_{1l} (m_D m_D^\dagger)_{1j} (m_D^*)_{jl} \right) \right) \frac{M_1}{M_j}. \quad (96)$$

Similarly, one has to consider the “wash-out mass parameter” for each flavour l , $\widetilde{m}_l \propto |(m_D)_{1l}|^2$, which depends on the decay rate of N_1 to the leptons of flavour l .

Since leptogenesis requires CPV, one can ask whether the one necessary to explain the baryon asymmetry is related to the CP-violating phases observable at low energies (in the PMNS mixing matrix) [163, 164]. As discussed in Sec. 6.2.4, in general see-saw models contain a larger number of parameters than those measurable. Consequently, in a completely model-independent way it is not possible to draw a direct link between the two. However, we are interested in models which aim to explain the values of neutrino masses and of the mixing structure we observe. As we briefly reviewed in Sec. 6.2.4, these models have a reduced number of parameters which can control both the high energy and low energy ones, see Sec. 6.3. In these scenarios, it is common for the low energy phases to be directly connected to the baryon asymmetry.

We can even make some more general statement. Let’s restrict the discussion to see-saw type I with three hierarchical heavy neutrino masses. In the one-flavour approximation, using the Casas-Ibarra approximation, one can show that the low energy U cancels out in the CP-asymmetry. This implies that it is possible to have low energy CP violation and no leptogenesis. However, this is not true if one considers flavour effects, see Eq. (96). The PMNS matrix does not cancel out in the CP asymmetry and the low energy CP-violating phases do induce a baryon asymmetry. It can also be shown that even δ can generate enough CPV to reproduce the observed baryon asymmetry. This is a highly non-trivial statement since its CPV effects are suppressed by θ_{13} . One can conclude that generically the observation of lepton number violation (e.g., neutrinoless double beta decay) and of CP violation in long-baseline neutrino oscillation experiments and/or possibly neutrinoless double beta decay would constitute a strong indication (even if not a proof) in favour of the leptogenesis mechanism as the origin of the baryon asymmetry of the Universe.

7 Neutrinos in the Early Universe and in Astrophysics

Thanks to their interactions, neutrinos were in thermal equilibrium with the rest of the plasma in the Early Universe. As the temperature T dropped, neutrinos decoupled when the interaction rate became too slow compared to the expansion of the Universe. Since then they travelled unperturbed redshifting their momentum but, due to their large density, they nevertheless affected significantly the evolution of the Universe leaving an imprint in Big Bang Nucleosynthesis, the Cosmic Microwave background, large scale structure (LSS) formation and finally pervading the Universe with a cosmic neutrino background of around 100 neutrinos per cm^3 .

7.1 Neutrino decoupling.

The SM interactions such as

$$\nu\bar{\nu} \leftrightarrow e^+e^-, \quad \nu e \leftrightarrow \nu e, \dots$$

kept neutrinos in thermal equilibrium at sufficiently high densities. They decouple when the interaction rate Γ becomes comparable with the expansion rate \mathcal{H} ,

$$\Gamma \sim \mathcal{H},$$

with $\Gamma \sim G_F^2 T^5$ and $\mathcal{H} \sim T^2/M_{\text{Pl}}$ in a radiation dominated era. This leads to a decoupling temperature $T_d \sim 1 \text{ MeV}$, which slightly differs for electron neutrinos, being lower, from that of μ - τ neutrinos as the former have both CC and NC interactions. Since we know from beta-decay measurements that neutrino masses must be below the eV scale, relic neutrinos decoupled while they were still relativistic.

7.2 Neutrino temperature.

Soon after neutrino decoupling, electrons-positrons get out of equilibrium transferring their entropy to the photon plasma. The neutrinos do not partake in this transfer and consequently they remain colder than the photons. Using entropy conservation, one can find that

$$\frac{T_\nu}{T_\gamma} = \left(\frac{4}{11} \right)^{1/3}.$$

7.3 Neutrinos as hot dark matter.

After decoupling, neutrinos have their momentum redshifted by the expansion of the Universe and turn non-relativistic at late times²⁴. An imprint of their existence is on the CMB and on LSS. At early times, massive neutrinos change the matter-radiation equality leading to a small shift and height increase of the peaks of the CMB power spectrum [156], due to the Sachs-Wolfe effect [165]. Later on, their biggest effect is that they behave as hot dark matter at the time of cosmological structure formation, suppressing their growth at small scales. These structures formed from initial seeds, i.e. perturbations in the dark matter density, under the gravitational pull. Cold dark matter falls into the gravitational wells which are created by the overdensities, making them grow further and leading to the formation of galaxies and clusters. Neutrinos were too fast to be trapped in the wells and free-streamed out of them, suppressing the growth of structures at sufficiently small scales. The neutrino free-streaming length λ_{FS} depends on their thermal velocity v_{th} as [166]

$$\lambda_{FS} = 2\pi \sqrt{\frac{2}{3}} \frac{v_{th}(t)}{\mathcal{H}(t)},$$

where $\mathcal{H}(t)$ is the Hubble rate at a given time t . We notice that the thermal velocity is inversely proportional to the neutrino mass. The suppression of the matter power spectrum at scales smaller than the free-streaming length is approximately given by

$$\frac{\Delta \mathcal{P}}{\mathcal{P}} \propto 8 \frac{\Omega_\nu}{\Omega_m}, \quad (97)$$

where Ω_m is the matter density fraction and Ω_ν the neutrino density fraction²⁵. The latter is related to neutrino masses as

$$\Omega_\nu = \sum_i m_i / (93 \text{ eV} h^2), \quad (98)$$

where h is defined as $h(t) \equiv \mathcal{H}(t)/(100 \text{ km s}^{-1} \text{ Mpc}^{-1})$. As these effects are purely gravitational, there is no distinction between the different mass states which all contribute in the same manner to a good approximation. As we know that at least two neutrinos are massive, we can set a lower limit on the sum of neutrino masses which depends on the neutrino mass ordering:

$$\begin{aligned} \sum_i m_i &> \sqrt{\Delta m_{21}^2} + \sqrt{\Delta m_{31}^2} \simeq 0.06 \text{ eV} \quad \text{for NO,} \\ \sum_i m_i &> \sqrt{|\Delta m_{31}^2|} + \sqrt{|\Delta m_{32}^2|} \simeq 0.10 \text{ eV} \quad \text{for IO.} \end{aligned}$$

²⁴As one of the neutrinos could be nearly massless, there is the possibility that one of the three massive neutrinos is still relativistic today.

²⁵ Ω_i is defined as the ratio of the density of particle i over the critical density of the universe ρ_c .

The distribution of structures in the Early Universe is measured with good accuracy, leading to a strong upper bound on the sum of neutrino masses. There are two main tools to establish the distribution of matter at the relevant scales:

- observing tracers of the matter distribution, e.g. galaxy surveys, such as SDSS [167], BOSS [168], HETDEX [169] and DES [170], or low density intergalactic gas for Ly- α surveys [171]. This type of measurement is very powerful but is affected by the problem of bias, i.e. the relation between the matter and the tracer power spectra;
- looking directly at the dark matter distribution via gravitational lensing [172]. This is becoming more and more the tool of choice for constraining the matter power spectrum and consequently neutrino masses.

Although cosmology provides the most stringent constraints on neutrino masses, care should be given to the fact that the bounds can vary depending on the set of cosmological data included and one needs to exploit the complementarity between different probes, for instance high and low red-shift observables, to break the degeneracy with other cosmological parameters. We just note that there is currently some tension in the measured value of H_0 by Planck and SN surveys, with a possible impact on neutrino parameters. Importantly, the bounds on neutrino masses are obtained assuming the standard Λ CDM model. Different underlying cosmological models, e.g. invoked to explain the accelerated expansion of the Universe, could lead to significantly different constraints. Without entering in this complex discussion, we report the bound obtained by the combination of Planck CMB and BOSS BAO [156]

$$\sum_i m_i < 0.12 \text{ eV} \quad (95\% \text{ C.L.}).$$

In the literature other recent bounds typically are around 0.15–0.3 eV depending on the datasets included. Therefore, as current and future cosmological measurements continue to improve their precision, it is expected that cosmology will be able to distinguish between the NO and IO ordering of masses. It will be particularly interesting to assess the reliability of such bounds and to combine them with terrestrial experiments, such as neutrinoless double beta decay and direct mass searches, see Sec. 5.2.

7.4 Sterile neutrinos as warm dark matter

Light nearly-sterile neutrinos ν_h with masses in the keV range have been advocated as dark matter candidates. If the mixing angle between the nearly-sterile neutrino and the active neutrino is large, these particles were in thermal equilibrium in the Early Universe and decoupled at a temperature slightly higher than that of standard neutrinos. For small mixing angles, they were produced via oscillations in neutrino processes without ever reaching thermal equilibrium [173].

These particles can decay into 3ν via SM NC interactions, further suppressed by the mixing angle squared. If their mass is in the keV range, they are quasi-stable on cosmological timescales and they can constitute the dominant component of DM. The production of nearly-sterile neutrinos can be obtained by solving the Boltzmann equation for the nearly-sterile neutrino phase space density f_h [173, 174]

$$\left(\frac{\partial f_h}{\partial T}\right)_{E/T} = \frac{1}{4} \frac{1}{\mathcal{H}T} \Gamma_\alpha \sin^2 2\theta_m (f_\alpha - f_h),$$

where $\left(\frac{\partial f_h}{\partial T}\right)_{E/T}$ is the derivative taken at constant E/T , $\mathcal{H} = 5.4 T^2/M_{Pl}$, with the Plank mass $M_{Pl} = 1.2 \times 10^{19}$ GeV, Γ_α is the ν_α interaction rate $\Gamma_\alpha \sim G_F^2 T^4 E$ and $f_\alpha = (1 + \exp(E/T))^{-1}$ is the phase space density for active neutrinos. $\sin^2 2\theta_m$ denotes the mixing angle in the thermal bath which is related to the one in vacuum θ as

$$\sin^2 2\theta_m \simeq \frac{\left(\frac{m_A^2}{2E}\right)^2 \sin^2 2\theta}{\left(\frac{m_A^2}{2E} + 1.1 \times 10^{-8} T^4 E/\text{GeV}^4\right)^2}. \quad (99)$$

The contribution of the nearly-sterile neutrino to the energy density is given by $\rho_h = m_h n_h$, where n_h is the number density obtained integrating f_h . Other mechanisms of production invoke a lepton asymmetry which can resonantly enhance the angle θ_m and lead to a colder spectrum or assume late decays of heavier particles giving a even colder distribution of sterile neutrinos. Depending on the spectrum, these nearly-sterile neutrinos can behave as cold, cool, warm dark matter leading to intermediate behaviour in structure formation [175]. Typically, the matter power spectrum is suppressed at small structures with a sharp cut-off in the linear matter power spectrum. Confronting these predictions with observations allows to set bounds on the nearly-sterile neutrino mass, given a specific production mechanism.

Apart from the decay into 3ν , ν_h can also subdominantly decay into a photon and a neutrino with a branching ratio of around 1%. This channel would give rise to a x-ray line with $E_\gamma = m_h/2$ which can be searched for by looking in DM-rich regions of the Universe, such as the centre of our Galaxy and DM-dominated dwarf galaxies.

7.5 Supernova neutrinos

During a supernova (SN) explosion, 99% of the energy is released in neutrinos as they can escape from deep regions thanks to their weak interactions [176]. One can identify three main phases of emission: the neutronization peak, the accretion phase and the cooling phase. The neutronization peak takes place in the first ~ 25 ms. Electron neutrinos are produced by electron capture on protons and nuclei. In the second phase, lasting tens to hundreds of milliseconds, the shock stalls before the start of the SN explosion. Mainly electron neutrinos are emitted and the spectrum can be rather complex due to the standing accretion shock instability. The final phase can last few tens of seconds and it is when the neutron star, born from the explosion, cools. Most of the SN gravitational binding energy is released in this phase. An intense flux of neutrinos and antineutrinos of all flavours is emitted with energies of tens of MeV. Because electron neutrinos interact more strongly with the background than electron antineutrinos, they are emitted from a neutrinosphere located less deep in the SN, implying a smaller energy. Similarly, as muon and tau neutrinos have only NC interactions with the background of electrons, protons and neutrons, their energy will be even higher. The hierarchy of average energies expected is $\langle E_{\nu_\mu, \nu_\tau} \rangle > \langle E_{\bar{\nu}_e} \rangle > \langle E_{\nu_e} \rangle$.

As the SN neutrinos propagate from the inner parts of the SN to the outer layers, their evolution is affected by oscillations in matter. Deep in the SN core, the neutrino density is so high that neutrinos become a background to themselves and a large matter potential due to neutrino-neutrino interactions is generated. ‘‘Collective oscillations’’ can take place as the entire neutrino system evolves as a single collective mode. Due to the complex matter profiles and time evolution, neutrino transition can be quite complex and present a behaviour which can vary significantly with energy, flavour and time. As SN neutrinos leave the inner parts of the SN, at smaller densities, SN neutrinos will feel the effects of the matter resonance due to Δm_{31}^2 and Δm_{21}^2 . Finally, they will travel through space reaching the Earth. Here, they may undergo additional transitions if they transverse a significant amount of matter.

SN neutrinos can be hunted for by several types of experiments [177]. Large Water-Cherenkov detectors, such as Super-Kamiokande, and liquid scintillators, e.g. KamLAND and the future SNO+ and JUNO, can detect mainly electron antineutrinos via inverse beta decay. The addition of gadolinium, already ongoing in Super-Kamiokande, significantly improves the neutron capture detection efficiency and reduces the backgrounds enhancing the sensitivity. Elastic scattering can also give an important, although much smaller, sample of neutrinos mainly of the electron flavour. NC and other interactions on nuclei give a small contribution to the number of events. LAr detectors, such as DUNE at SURF, have unique sensitivity to electron neutrinos via the reaction $\nu_e {}^{40}\text{Ar} \rightarrow e {}^{40}\text{K}^*$ and can detect antineutrinos via inverse beta decay and NC interactions.

On 24 February 1987 a bright supernova of type II was found in the Large Magellanic Cloud about 50 kpc away from the solar system [178]. It was named SN1987A. The neutrinos emitted by this supernova were observed at the neutrino detectors operating at the time: Kamiokande-II [179], IMB [180],

Baksan and LSD. They recorded few tens of events in a time window of 10 seconds few hours before the optical discovery of SN1987A ²⁶. Their observation allows to set bounds on neutrino properties. Their mass can be bound requiring that the spread in time of the events does not exceed few seconds. This translates into a bound of around 5-30 eV, depending on the neutrino emission assumptions. Moreover, they imply that a large fraction of the SN energy was emitted in neutrinos, limiting the amount which can be carried away by other invisible particles and therefore constraining neutrino interactions in extensions of the Standard Model, their decay time and their mixing with heavy neutrinos. The observation of the SN1987A neutrinos marked the start of extrasolar system neutrino astronomy. M. Koshiba received the Nobel Prize in Physics in 2012 for this discovery.

8 Conclusions and Outlook

Thanks to an impressive series of experiments, we have established that neutrino oscillate. This discovery is of ground breaking importance as it implies that neutrinos have mass and mix and constitute the first, and so far only, particle physics evidence that the SM is incomplete. The two key questions, possibly inter-related, which emerge concern the origin of neutrino masses and the principle behind the observed leptonic structure. In order to address them, we require a picture of neutrino properties as complete and as precise as possible. This means identifying the nature of neutrinos, establishing the absolute values of neutrino masses, by determining their ordering and the mass scale, measuring the mixing angles and the CP violating phase very precisely, and testing if the standard 3-neutrino mixing scenario is correct. Despite being challenging, an exciting experimental programme is ongoing and planned for the future and will be able to address these issues. In these lectures I have reviewed the phenomenology relevant in current and future neutrino experiments, the theory behind neutrino masses and mixing and the impact of neutrinos in the Early Universe, from leptogenesis to dark matter.

9 Acknowledgements

I would like to express my heartfelt thanks to the students and the organisers of the 2018 CERN-JINR European School of High-Energy Physics for the fantastic scientific atmosphere. I would also like to thank Arsenii Titov for careful reading of the manuscript and the NuFIT collaboration (<http://www.nu-fit.org>) for kindly providing the plots for Fig. 4. This work was partially supported by the European Research Council under ERC Grant NuMass (FP7-IDEAS-ERC ERC-CG 617143) and by the European Union's Horizon 2020 research and innovation programme under the Marie Skłodowska-Curie grant agreement No. 690575 (RISE InvisiblesPlus) and No. 674896 (ITN Elusives). I acknowledge partial support from the Wolfson Foundation and the Royal Society.

References

- [1] <https://www.symmetrymagazine.org/article/march-2007/neutrino-invention>. See also *Cambridge Monogr. Part. Phys. Nucl. Phys. Cosmol.*, **14** (2000) 1.
- [2] J. Chadwick, *Nature* **129** (1932) 312.
- [3] E. Fermi, *Nuovo Cim.* **11** (1934) 1.
- [4] H. Bethe and R. Peierls, *Nature* **133** (1934) 532.
- [5] See, B. Pontecorvo, *Cambridge Monogr. Part. Phys. Nucl. Phys. Cosmol.*, **1** (1991) 25.
- [6] F. Reines and C. L. Cowan, *Nature* **178** (1956) 446; C. L. Cowan *et al.*, *Science* **124** (1956) 103.
- [7] T. D. Lee and C.-N. Yang, *Phys. Rev.* **104** (1956) 254.
- [8] C. S. Wu *et al.*, *Phys. Rev.* **105** (1957) 1413.

²⁶The LSD events were recorded 5 hours before those of the other three detectors and their origin remains controversial. The Baksan Underground Scintillation Telescope could not provide an independent observation due to the low statistics but when supplemented with information from the other two detectors they could identify around 5 events in the relevant time window.

- [9] M. Goldhaber, L. Grodzins and A. W. Sunyar, *Phys. Rev.* **109** (1958) 1015.
- [10] L. Landau, *Nucl. Phys.* **3** (1957) 127.
- [11] T. D. Lee and C. N. Yang, *Phys. Rev.* **105** (1957) 1671.
- [12] A. Salam, *Nuovo Cim.* **5** (1957) 299.
- [13] S. L. Glashow, *Nucl. Phys.* **22** (1961) 579.
- [14] S. Weinberg, *Phys. Rev. Lett.* **19** (1967) 1264.
- [15] A. Salam, Proc. of the 8th Nobel Symposium on “Elementary Particle Theory, Relativistic Groups and Analyticity”, Stockholm, Sweden, 1968, edited by N. Svartholm, p. 367.
- [16] E. Majorana, *Nuovo Cim.* **14** (1937) 171.
- [17] E. J. Konopinski and H. M. Mahmoud, *Phys. Rev.* **92** (1953) 1045.
- [18] J. C. Street and E. C. Stevenson, *Phys. Rev.* **52** (1937) 1003.
- [19] S. H. Neddermeyer and C. D. Anderson, *Phys. Rev.* **51** (1937) 884.
- [20] B. Pontecorvo, *Sov. Phys. JETP* **10** (1960) 1236.
- [21] G. Danby *et al.*, *Phys. Rev. Lett.* **9** (1962) 36.
- [22] K. Kodama *et al.* (DONUT Collaboration), *Phys. Lett.* **B 504** (2001) 218.
- [23] B. Pontecorvo, *Sov. Phys. JETP* **6** (1957) 429; B. Pontecorvo, *Sov. Phys. JETP* **7** (1958) 172.
- [24] Z. Maki, M. Nakagawa and S. Sakata, *Prog. Theor. Phys.* **28** (1962) 870.
- [25] B. Pontecorvo, *Sov. Phys. JETP* **26** (1968) 984.
- [26] V. N. Gribov and B. Pontecorvo, *Phys. Lett.* **B28** (1969) 493.
- [27] S. Eliezer and A. R. Swift, *Nucl. Phys.* **B105** (1976) 45; H. Fritzsch and P. Minkowski, *Phys. Lett.* **B62** (1976) 72; S. M. Bilenky and B. Pontecorvo, *Sov. J. Nucl. Phys.* **24** (1976) 316; S. M. Bilenky and B. Pontecorvo, *Nuovo Cim. Lett.* **17** (1976) 569.
- [28] B. T. Cleveland *et al.*, and J. Ullman, *Astrophys. J.* **496** (1998) 505.
- [29] J. N. Bahcall, M. H. Pinsonneault, and S. Basu, *Astrophys. J.* **555** (2001) 990.
- [30] W. Hampel *et al.*, *Phys. Lett.* **B447** (1999) 127.
- [31] J. N. Abdurashitov *et al.*, *J. Exp. Theor. Phys.* **95** (2002) 181 [*Zh. Eksp. Teor. Fiz.* **122** (2002) 211].
- [32] Y. Fukuda *et al.*, *Phys. Rev. Lett.* **77** (1996) 1683.
- [33] Y. Fukuda *et al.*, *Phys. Rev. Lett.* **82** (1999) 2430.
- [34] Q. R. Ahmad *et al.*, *Phys. Rev. Lett.* **87** (2001) 071301; Q. R. Ahmad *et al.*, *Phys. Rev. Lett.* **89** (2002) 011301.
- [35] K. Eguchi *et al.*, *Phys. Rev. Lett.* **90** (2003) 021802.
- [36] C. V. Achar *et al.*, *Phys. Lett.* **18** (1965) 196; C. V. Achar *et al.*, *Phys. Lett.* **19** (1965) 78.
- [37] F. Reines *et al.*, *Phys. Rev. Lett.* **15** (1965) 429.
- [38] See e.g. T. J. Haines *et al.*, *Phys. Rev. Lett.* **57** (1986) 1986; K. S. Hirata *et al.*, *Phys. Lett.* **B205** (1988) 416; Y. Fukuda *et al.*, *Phys. Lett.* **B335** (1994) 237; W. W. M. Allison *et al.*, *Phys. Lett.* **B391** (1997) 491429; S. P. Ahlen *et al.*, *Phys. Lett.* **B357** (1995) 481; M. Ambrosio *et al.*, *Phys. Lett.* **B434** (1998) 451.
- [39] Y. Fukuda *et al.*, *Phys. Rev. Lett.* **81** (1998) 1562.
- [40] M. Tanabashi *et al.* (Particle Data Group), *Phys. Rev.* **D 98** (2018) 030001.
- [41] S. M. Bilenky, J. Hosek and S. T. Petcov, *Phys. Lett.* **B94** (1980) 495.
- [42] J. Schechter and J. W. F. Valle, *Phys. Rev.* **D22** (1980) 2227; M. Doi *et al.*, *Phys. Lett.* **B102** (1981) 323.
- [43] C. Jarlskog, *Phys. Rev. Lett.* **55** (1985) 1039; C. Jarlskog, *Z. Phys.* **C29** (1985) 491; O. W. Greenberg, *Phys. Rev. D* **32** (1985) 1841; I. Dunitz, O. W. Greenberg and D. d. Wu, *Phys. Rev. Lett.* **55** (1985) 2935.

- [44] For initial discussions of this issue, see S. Nussinov, *Phys. Lett.* **B63** (1976) 201; B. Kayser, *Phys. Rev. D* **24** (1981) 110; K. Kiers, S. Nussinov and N. Weiss, *Phys. Rev.* **D53** (1996) 537.
- [45] E. K. Akhmedov and A. Yu. Smirnov, *Phys. Atom. Nucl.* **72** (2009) 1363; E. K. Akhmedov and J. Kopp, *JHEP* **04** (2010) 008 [Erratum: *JHEP* **10** (2013) 052].
- [46] F. P. An *et al.*, *Phys. Rev. Lett.* **108** (2012) 171803.
- [47] J. K. Ahn *et al.*, *Phys. Rev. Lett.* **108** (2012) 191802.
- [48] Y. Abe *et al.*, *Phys. Rev. Lett.* **108** (2012) 131801.
- [49] S. Abe *et al.*, *Phys. Rev. Lett.* **100** (2008) 221803.
- [50] L. Wolfenstein, *Phys. Rev.* **D17** (1978) 2369.
- [51] S. P. Mikheev and A. Yu. Smirnov, *Sov. J. Nucl. Phys.* **42** (1985) 913 [*Yad. Fiz.* **42** (1985) 1441].
- [52] A. Cervera *et al.*, *Nucl. Phys. B* **579** (2000) 17 [Erratum: *Nucl. Phys. B* **593** (2001) 731]; M. Freund, *Phys. Rev. D* **64** (2001) 053003; E. K. Akhmedov *et al.*, *JHEP* **0404** (2004) 078.
- [53] K. Abe *et al.* [Super-Kamiokande Collaboration], *Phys. Rev. D* **97** (2018) 072001.
- [54] P. Adamson *et al.* [MINOS Collaboration], *Phys. Rev. Lett.* **110** (2013) 251801;
- [55] M. G. Aartsen *et al.* [IceCube Collaboration], *Phys. Rev. D* **91** (2015) no.7, 072004
- [56] P. Adamson *et al.* [MINOS Collaboration], *Phys. Rev. Lett.* **110** (2013) 171801.
- [57] K. Abe *et al.* [T2K Collaboration], *Phys. Rev. Lett.* **107** (2011) 041801. K. Abe *et al.* [T2K Collaboration], *Phys. Rev. Lett.* **118** (2017) 151801; K. Abe *et al.* [T2K Collaboration], *Phys. Rev. Lett.* **121** (2018) 171802.
- [58] D. S. Ayres *et al.* [NOvA Collaboration], hep-ex/0503053; P. Adamson *et al.* [NOvA Collaboration], *Phys. Rev. Lett.* **118** (2017) 151802; M. A. Acero *et al.* [NOvA Collaboration], *Phys. Rev. D* **98** (2018) 032012.
- [59] N. Agafonova *et al.* [OPERA Collaboration], *Phys. Rev. Lett.* **120** (2018) 211801 [Erratum: *Phys. Rev. Lett.* **121** (2018) 139901].
- [60] K. Abe *et al.* [Super-Kamiokande Collaboration], *Phys. Rev. D* **94** (2016) 052010.
- [61] B. Aharmim *et al.* [SNO collaboration], *Phys. Rev.* **C88** (2013) 025501.
- [62] G. Bellini *et al.* [Borexino Collaboration], *Phys. Rev. D* **82** (2010) 033006; G. Bellini *et al.*, *Phys. Rev. Lett.* **107** (2011) 141302; M. Agostini *et al.* [BOREXINO Collaboration], *Nature* **562** (2018) 505.
- [63] D. Adey *et al.* [Daya Bay Collaboration], *Phys. Rev. Lett.* **121** (2018) 241805.
- [64] G. Bak *et al.* [RENO Collaboration], *Phys. Rev. Lett.* **121** (2018) 201801.
- [65] Y. Abe *et al.* [Double Chooz Collaboration], *JHEP* **1410** (2014) 086 [Erratum: *JHEP* **1502** (2015) 074].
- [66] A. Gando *et al.* [KamLAND Collaboration], *Phys. Rev. D* **88** (2013) 033001.
- [67] C. Athanassopoulos *et al.* (LSND Collaboration), *Phys.Rev. Lett.* **75** (1995) 2650; C. Athanassopoulos *et al.* (LSND Collaboration), *Phys.Rev. Lett.* **77** (1996) 3082.
- [68] A. A. Aguilar-Arevalo *et al.* (MiniBooNE), *Phys.Rev. Lett.* **102** (2009) 101802; A. A. Aguilar-Arevalo *et al.* (MiniBooNE), *Phys. Rev. Lett.* **121** (2018) 221801.
- [69] P. Ballett, S. Pascoli and M. Ross-Lonergan, *Phys. Rev. D* **99** (2019) 071701.
- [70] J. Kopp, M. Maltoni, and T. Schwetz, *Phys.Rev. Lett.* **107** (2011) 091801; M. Dentler *et al.*, *JHEP* **1808** (2018) 010; S. Gariazzo *et al.*, *JHEP* **06** (2017) 135; G. H. Collin *et al.*, *Phys.Rev. Lett.* **117** (2016) 221801.
- [71] T. Mueller *et al.*, *Phys. Rev.* **C83** (2011) 054615; P. Huber, *Phys. Rev.* **C84** (2011) 024617; G. Mention *et al.*, *Phys. Rev.* **D83** (2011) 073006.
- [72] M. A. Acero, C. Giunti, and M. Laveder, *Phys. Rev.* **D78** (2008) 073009; C. Giunti and M. Laveder, *Phys. Rev.* **C83** (2011) 065504.

- [73] M. Antonello *et al.* (LAr1-ND, ICARUS-WA104, MicroBooNE), arXiv:1503.01520 [physics.ins-det]; D. Cianci *et al.*, *Phys. Rev.* **D96**, 055001 (2017).
- [74] I. Esteban *et al.*, *JHEP* **01** (2019) 106, NuFIT 4.1 (2019), www.nu-fit.org. See also, F. Capozzi, E. Lisi, A. Marrone and A. Palazzo, *Prog. Part. Nucl. Phys.* **102** (2018) 48 and 2019 update reported by E. Lisi at CERN Council Open Symposium on the Update of European Strategy for Particle Physics, 13-16 May 2019, Granada, Spain, <https://indico.cern.ch/event/808335/>
- [75] C. Adams *et al.* [LBNE Collaboration], arXiv:1307.7335 [hep-ex]; R. Acciarri *et al.* [DUNE Collaboration], arXiv:1601.05471 [physics.ins-det]; R. Acciarri *et al.* [DUNE Collaboration], arXiv:1512.06148 [physics.ins-det].
- [76] K. Abe *et al.*, arXiv:1109.3262 [hep-ex]; K. Abe *et al.* [Hyper-Kamiokande Proto-Coll.], *PTEP* **2015** (2015) 053C02.
- [77] M. Ishitsuka, T. Kajita, H. Minakata and H. Nunokawa, *Phys. Rev. D* **72** (2005) 033003; K. Abe *et al.* [Hyper-Kamiokande proto-Collaboration], *PTEP* **2018** (2018) 063C01.
- [78] E. Baussan *et al.* [ESSnuSB Collaboration], *Nucl. Phys. B* **885** (2014) 127; E. Baussan *et al.* [ESSnuSB Collaboration], arXiv:1212.5048 [hep-ex].
- [79] S. Geer, *Phys. Rev. D* **57** (1998) 6989 [Erratum: *Phys. Rev. D* **59** (1999) 039903]; A. De Rujula, M. B. Gavela and P. Hernandez, *Nucl. Phys. B* **547** (1999) 21; S. Geer, O. Mena and S. Pascoli, *Phys. Rev. D* **75** (2007) 093001; S. Choubey *et al.* [IDS-NF Collaboration], arXiv:1112.2853 [hep-ex].
- [80] C. Aberle *et al.*, arXiv:1307.2949 [physics.acc-ph].
- [81] S. Razzaque and A. Y. Smirnov, *JHEP* **1505** (2015) 139.
- [82] U. F. Katz [KM3NeT Collaboration], arXiv:1402.1022 [astro-ph.IM]; A. Domi *et al.* [KM3NeT Collaboration], *EPJ Web Conf.* **207** (2019) 04003.
- [83] M. G. Aartsen *et al.* [IceCube Collaboration], *J. Phys. G* **44** (2017) 054006.
- [84] F. An *et al.*, *J. Phys. G* **43** (2016) 030401.
- [85] S. T. Petcov and M. Piai, *Phys. Lett. B* **533** (2002) 94.
- [86] S. Choubey, S. T. Petcov and M. Piai, *Phys. Rev. D* **68** (2003) 113006.
- [87] M. Goeppert-Mayer, *Phys. Rev.* **48** (1935) 512.
- [88] W. Furry, *Phys. Rev.* **56** (1939) 1184.
- [89] S. M. Bilenky, S. Pascoli and S. T. Petcov, *Phys. Rev.* **D64** (2001) 053010; S. Pascoli and S. T. Petcov, *Phys. Lett. B* **544** (2002) 239.
- [90] S. M. Bilenky *et al.*, *Phys. Rev.* **D54** (1996) 4432; S. M. Bilenky *et al.*, *Phys. Lett. B* **465** (1999) 193; V. Barger and K. Whisnant, *Phys. Lett. B* **456** (1999) 194.
- [91] F. Vissani, *JHEP* **9906** (1999) 022; W. Rodejohann, *Phys. Rev. D* **62** (2000) 013011; H. V. Klapdor-Kleingrothaus, H. Pas and A. Y. Smirnov, *Phys. Rev. D* **63** (2001) 073005; F. Feruglio, A. Strumia and F. Vissani, *Nucl. Phys. B* **637** (2002) 345 [Addendum: *Nucl. Phys. B* **659** (2003) 359].
- [92] H. Nunokawa, W. J. C. Teves and R. Zukanovich Funchal, *Phys. Rev. D* **66** (2002) 093010.
- [93] S. Pascoli, S. T. Petcov and W. Rodejohann, *Phys. Lett. B* **558** (2003) 141.
- [94] S. Pascoli, S. T. Petcov and L. Wolfenstein, *Phys. Lett. B* **524** (2002) 319; V. Barger, S. L. Glashow, P. Langacker and D. Marfatia, *Phys. Lett. B* **540** (2002) 247; H. Nunokawa, W. J. C. Teves and R. Zukanovich Funchal, *Phys. Rev. D* **66** (2002) 093010.
- [95] M. G. Inghram and J. H. Reynolds, *Phys. Rev.* **78** (1950) 822.
- [96] S. R. Elliott, A. A. Hahn and M. K. Moe, *Phys. Rev. Lett.* **59** (1987) 2020.
- [97] A. Gando *et al.* [KamLAND-Zen Collaboration], *Phys. Rev. Lett.* **117** (2016) 082503 [Addendum: *Phys. Rev. Lett.* **117** (2016) 109903].
- [98] V. Fischer [SNO+ Collaboration], arXiv:1809.05986 [physics.ins-det].

- [99] J. B. Albert *et al.* [EXO-200 Collaboration], *Nature* **510** (2014) 229; J. B. Albert *et al.* [EXO Collaboration], *Phys. Rev. Lett.* **120** (2018) 072701.
- [100] J. B. Albert *et al.* [nEXO Collaboration], *Phys. Rev. C* **97** (2018) 065503.
- [101] D. Nygren, *Nucl. Instrum. Meth. A* **603** (2009) 337; J. J. Gomez-Cadenas *et al.* [NEXT Collaboration], *Adv. High Energy Phys.* **2014** (2014) 907067; J. Martín-Albo *et al.* [NEXT Collaboration], *JHEP* **1605** (2016) 159.
- [102] X. Chen *et al.*, *Sci. China Phys. Mech. Astron.* **60** (2017) 061011; K. Han [PandaX-III Collaboration], arXiv:1710.08908 [physics.ins-det].
- [103] M. Agostini *et al.* [GERDA Collaboration], *Phys. Rev. Lett.* **120** (2018) 132503; M. Agostini *et al.* [GERDA Collaboration], *Eur. Phys. J. C* **78** (2018) 388.
- [104] S. I. Alvis *et al.* [Majorana Collaboration], arXiv:1902.02299 [nucl-ex].
- [105] N. Abgrall *et al.*, *AIP Conf. Proc.* **1894** (2017) 020027.
- [106] C. Alduino *et al.* [CUORE Collaboration], *Phys. Rev. Lett.* **120** (2018) 132501.
- [107] [CUPID Interest Group], arXiv:1907.09376 [physics.ins-det].
- [108] E. Fermi, *Ricerca Scientifica* **2** (1933) 12; E. Fermi, *Z. Phys.* **88** (1934) 161.
- [109] F. Perrin, *Comptes Rendues* **197** (1933) 1625.
- [110] J. Wolf [KATRIN Collaboration], *Nucl. Instrum. Meth. A* **623** (2010) 442; V. Sibille [Katrin Collaboration], *PoS NOW* **2018** (2019) 072.
- [111] S. Weinberg, *Phys. Rev. Lett.* **43** (1979) 1566.
- [112] P. Minkowski, *Phys. Lett. B* **67** (1977) 421; M. Gell-Mann, P. Ramond, and R. Slansky in *Supergravity*, p. 315, edited by F. Nieuwenhuizen and D. Friedman, North Holland, Amsterdam, 1979; T. Yanagida, Proc. of the *Workshop on Unified Theories and the Baryon Number of the Universe*, edited by O. Sawada and A. Sugamoto, KEK, Japan 1979; R.N. Mohapatra, G. Senjanovic, *Phys. Rev. Lett.* **44**, (1980) 912.
- [113] M. Magg and C. Wetterich, *Phys. Lett.* **B94** (1980) 61; J. Schechter and J. W. F. Valle, *Phys. Rev.* **D22** (1980) 2227; C. Wetterich, *Nucl. Phys.* **B187**, (1981) 343; G. Lazarides, Q. Shafi, and C. Wetterich, *Nucl. Phys.* **B181** (1981) 287; R. N. Mohapatra and G. Senjanovic, *Phys. Rev.* **D23** (1981) 165.
- [114] R. Foot, H. Lew, X. G. He, and G. C. Joshi, *Z. Phys.* **C44** (1989) 441; E. Ma, *Phys. Rev. Lett.* **81** (1998) 1171.
- [115] F. Vissani, *Phys. Rev.* **D57** (1998) 7027; J. A. Casas, J. R. Espinosa, and I. Hidalgo, *JHEP* **11** (2004) 057, 2004; J. D. Clarke, R. Foot and R. R. Volkas, *Phys. Rev.* **D91** (2015) 073009; I. Brivio and M. Trott, *Phys. Rev. Lett.* **119** (2017) 141801.
- [116] F. del Aguila and J. A. Aguilar-Saavedra, *Nucl. Phys. B* **813** (2009) 22; P. S. B. Dev, A. Pilaftsis, and U.-k. Yang, *Phys. Rev. Lett.* **112** (2014) 081801; Y. Cai, T. Han, T. Li and R. Ruiz, *Front. in Phys.* **6** (2018) 40.
- [117] A. Atre, T. Han, S. Pascoli and B. Zhang, *JHEP* **0905** (2009) 030.
- [118] R. Aaij *et al.* [LHCb Collaboration], *Phys. Rev. Lett.* **112** (2014) 131802.
- [119] G. Aad *et al.* [ATLAS Collaboration], *JHEP* **1507** (2015) 162.
- [120] V. Khachatryan *et al.* [CMS Collaboration], *Phys. Lett. B* **748** (2015) 144; A. M. Sirunyan *et al.* [CMS Collaboration], *Phys. Rev. Lett.* **120** (2018) 221801; A. M. Sirunyan *et al.* [CMS Collaboration], *JHEP* **1901** (2019) 122.
- [121] D. Liventsev *et al.* [Belle Collaboration], *Phys. Rev. D* **87** (2013) 071102 [Erratum: *Phys. Rev. D* **95** (2017) 099903].
- [122] For a comprehensive review see e.g. K. N. Abazajian *et al.*, arXiv:1204.5379 [hep-ph]; M. Drewes *et al.*, *JCAP* **1701** (2017) 025.

- [123] R. E. Shrock, *Nucl. Phys.* **B206** (1982) 359; R. E. Shrock, *Phys. Rev. D* **24** (1981) 1232; R. E. Shrock, *Phys. Rev. D* **24** (1981) 1275.
- [124] D. Britton *et al.*, *Phys. Rev.* **D46** (1992) 885; T. Yamazaki *et al.*, *Conf. Proc.* **C840719** (1984) 262; A. Aoki *et al.*, *Phys. Rev.* **D84** (2011) 052002; A.V. Artamonov *et al.* (BNL E949 Collaboration), *Phys. Rev.* **D91** (2015) 052001.
- [125] For a compilation of previous bounds see A. Kusenko, S. Pascoli and D. Semikoz, *JHEP* **0511** (2005) 028.
- [126] C. Lazzeroni *et al.* (NA62 Collaboration), *Phys. Lett.* **B772** (2017) 712; E. Cortina Gil *et al.* [NA62 Collaboration], *Phys. Lett. B* **778** (2018) 137; L. Peruzzo [NA48/2 and NA62 Collaborations], *EPJ Web Conf.* **182** (2018) 02095.
- [127] M. Gronau, C. N. Leung, and J. L. Rosner, *Phys. Rev.* **D29** (1984) 2539; D. Gorbunov and M. Shaposhnikov, *JHEP* **10** (2007) 015.
- [128] G. Bernardi *et al.*, *Phys. Lett.* **166B** (1986) 479; G. Bernardi *et al.*, *Phys. Lett.* **B 203** (1988) 332.
- [129] A. Izmaylov and S. Suvorov, *Phys. Part. Nucl.* **48** (2017) 984.
- [130] P. Ballett, T. Boschi and S. Pascoli, arXiv:1905.00284 [hep-ph]; S. Alekhin *et al.*, *Rept. Prog. Phys.* **79** (2016) 124201; C. Ahdida *et al.* [SHiP Collaboration], *JHEP* **1904** (2019) 077.
- [131] L. S. Littenberg and R. Shrock, *Phys. Lett.* **B 491** (2000) 285.
- [132] E. K. Akhmedov, V. A. Rubakov and A. Y. Smirnov, *Phys. Rev. Lett.* **81** (1998) 1359.
- [133] T. Asaka and M. Shaposhnikov, *Phys. Lett.* **B 620** (2005) 17; P. Hernández *et al.*, *JHEP* **1510** (2015) 067; T. Hambye and D. Teresi, *Phys. Rev. Lett.* **117** (2016) 091801; P. Hernández *et al.*, *JHEP* **1608** (2016) 157; T. Hambye and D. Teresi, *Phys. Rev. D* **96** (2017) 015031; M. Drewes *et al.*, *Int. J. Mod. Phys. A* **33** (2018)1842002.
- [134] A. Zee, *Phys. Lett.* **93B** (1980) 389; T. P. Cheng and L. F. Li, *Phys. Rev.* **D22** (1980) 2860; A. Zee, *Nucl. Phys.* **B 264** (1986) 99; K. S. Babu, *Phys. Lett.* **B203** (1988) 132.
- [135] L. Hall and M. Suzuki, *Nuc. Phys.* **B231** (1984) 419; D. Chang and R. N. Mohapatra, *Phys. Rev. Lett.* **58** (1987) 1600; E. Ma, *Phys. Rev.* **D73** (2006) 077301.
- [136] P. S. B. Dev and A. Pilaftsis, *Phys. Rev.* **D86** (2012) 113001; Y. Zhang, X. Ji, and R. N. Mohapatra, *JHEP* **10** (2013) 104; P. Ballett, M. Hostert and S. Pascoli, *Phys. Rev. D* **99** (2019) 091701.
- [137] D. Wyler and L. Wolfenstein, *Nuc. Phys.* **B218** (1983) 205; R. N. Mohapatra and J. W. F. Valle, *Phys. Rev.* **D34** (1986) 1642; M. C. Gonzalez-Garcia and J. W. F. Valle, *Phys. Lett.* **B216** (1989) 360; G. C. Branco, W. Grimus, and L. Lavoura, *Nuc. Phys.* **B312** (1989) 492; E. K. Akhmedov, M. Lindner, E. Schnapka, and J. W. F. Valle, *Phys. Lett.* **B368** (1996) 270; *Phys. Rev.* **D53** (1996) 2752; J. Kersten and A. Yu. Smirnov, *Phys. Rev.* **D76** (2007) 073005; M. B. Gavela *et al.*, *JHEP* **09** (2009) 038; J. Barry, W. Rodejohann, and H. Zhang, *JHEP* **07** (2011) 091; H. Zhang, *Phys. Lett.* **B714** (2012) 262.
- [138] J. A. Casas and A. Ibarra, *Nucl. Phys.* **B618** (2001) 171.
- [139] P. F. Harrison, D. H. Perkins and W. G. Scott, *Phys. Lett.* **B 530** (2002) 167. Also, P. F. Harrison and W. G. Scott, *Phys. Lett.* **B 535** (2002) 163; Z. Z. Xing, *Phys. Lett.* **B 533** (2002) 85.
- [140] M. Fukugita, M. Tanimoto and T. Yanagida, *Phys. Rev. D* **57** (1998) 4429; V. D. Barger, S. Pakvasa, T. J. Weiler and K. Whisnant, *Phys. Lett.* **B 437** (1998) 107; S. Davidson and S. F. King, *Phys. Lett.* **B 445** (1998) 191; G. Altarelli, F. Feruglio and L. Merlo, *JHEP* **0905** (2009) 020; D. Meloni, *JHEP* **1110** (2011) 010.
- [141] See e.g. for the golden ratio, A. Datta, F. S. Ling and P. Ramond, *Nucl. Phys.* **B 671** (2003) 383; L. L. Everett and A. J. Stuart, *Phys. Rev. D* **79** (2009) 085005; F. Feruglio and A. Paris, *JHEP* **1103** (2011) 101; W. Rodejohann, *Phys. Lett.* **B 671** (2009) 267; A. Adulpravitchai, A. Blum and W. Rodejohann, *New J. Phys.* **11** (2009) 063026.
- [142] L. J. Hall, H. Murayama and N. Weiner, *Phys. Rev. Lett.* **84** (2000) 2572; A. de Gouvea and

- H. Murayama, *Phys. Lett. B* **747** (2015) 479.
- [143] G. Altarelli and F. Feruglio, *Rev. Mod. Phys.* **82** (2010) 2701; S. F. King and C. Luhn, *Rept. Prog. Phys.* **76** (2013) 056201.
- [144] R. Alonso *et al.*, *JHEP* **1311** (2013) 187.
- [145] S. F. King, *JHEP* **0508** (2005) 105.
- [146] C. S. Lam, *Phys. Lett. B* **656** (2007) 193; A. Blum, C. Hagedorn and M. Lindner, *Phys. Rev. D* **77** (2008) 076004; C. S. Lam, *Phys. Rev. D* **78** (2008) 073015.
- [147] See e.g. S. F. King, *JHEP* **0209** (2002) 011; P. H. Frampton, S. T. Petcov and W. Rodejohann, *Nucl. Phys. B* **687** (2004) 31; G. Altarelli, F. Feruglio and I. Masina, *Nucl. Phys. B* **689** (2004) 157; R. N. Mohapatra and W. Rodejohann, *Phys. Rev. D* **72** (2005) 053001; S. Antusch and S. F. King, *Phys. Lett. B* **631** (2005) 42; K. A. Hochmuth, S. T. Petcov and W. Rodejohann, *Phys. Lett. B* **654** (2007) 177.
- [148] See e.g. S. F. King, *Phys. Lett. B* **659** (2008) 244; Y. Shimizu, M. Tanimoto and A. Watanabe, *Prog. Theor. Phys.* **126** (2011) 81; S. F. King and C. Luhn, *JHEP* **1109** (2011) 042.
- [149] S. Antusch and S. F. King, *Phys. Lett. B* **591** (2004) 104; I. Masina, *Phys. Lett. B* **633** (2006) 134.
- [150] S. Antusch, P. Huber, S. F. King and T. Schwetz, *JHEP* **0704** (2007) 060.
- [151] G. Altarelli, P. A. N. Machado and D. Meloni, *PoS CORFU 2014* (2015) 012.
- [152] S. T. Petcov, *Nucl. Phys. B* **892** (2015) 400; also, D. Marzocca, S. T. Petcov, A. Romanino and M. C. Sevilla, *JHEP* **1305** (2013) 073; P. Ballett *et al.*, *JHEP* **1412** (2014) 122; I. Girardi, S. T. Petcov and A. V. Titov, *Nucl. Phys. B* **894** (2015) 733. .
- [153] F. Feruglio, C. Hagedorn and R. Ziegler, *JHEP* **1307** (2013) 027; F. Feruglio, C. Hagedorn and R. Ziegler, *Eur. Phys. J. C* **74** (2014) 2753; M. Holthausen, M. Lindner and M. A. Schmidt, *JHEP* **1304** (2013) 122; C. Hagedorn, A. Meroni and E. Molinaro, *Nucl. Phys. B* **891** (2015) 499.
- [154] M. C. Chen *et al.*, *Nucl. Phys. B* **883** (2014) 267.
- [155] W. Grimus and M. N. Rebelo, *Phys. Rept.* **281** (1997) 239.
- [156] N. Aghanim *et al.* [Planck Collaboration], arXiv:1807.06209 [astro-ph.CO].
- [157] A. D. Sakharov, *JTEP Lett.* **6** (1967) 24.
- [158] M. Fukugita and T. Yanagida, *Phys. Lett. B* **174** (1986) 45.
- [159] J. A. Harvey, M. S. Turner, *Phys. Rev. D* **42** (1990) 3344.
- [160] M. A. Luty, *Phys. Rev. D* **45** (1992) 455; M. Flanz, E. A. Paschos and U. Sarkar, *Phys. Lett. B* **345** (1995) 248 [Erratum-ibid. *B* **382** (1996) 447]; M. Plumacher, *Z. Phys. C* **74** (1997) 549.
- [161] L. Covi, E. Roulet and F. Vissani, *Phys. Lett. B* **384** (1996) 169; M. Flanz, E. A. Paschos, U. Sarkar and J. Weiss, *Phys. Lett. B* **389** (1996) 693; A. Pilaftsis, *Phys. Rev. D* **56** (1997) 5431; W. Buchmuller and M. Plumacher, *Phys. Lett. B* **431** (1998) 354.
- [162] R. Barbieri, P. Creminelli, A. Strumia and N. Tetradis, *Nucl. Phys. B* **575** (2000) 61; A. Abada *et al.*, *JCAP* **0604** (2006) 004; E. Nardi, Y. Nir, E. Roulet and J. Racker, *JHEP* **0601** (2006) 164; A. Abada *et al.*, *JHEP* **0609** (2006) 010.
- [163] See e.g. S. Davidson and A. Ibarra, *Nucl. Phys. B* **648** (2003) 345; G. C. Branco *et al.*, *Nucl. Phys. B* **640** (2002) 202; T. Endoh *et al.*, *Phys. Rev. Lett.* **89** (2002) 231601 .
- [164] S. Pascoli, S. T. Petcov and A. Riotto, *Phys. Rev. D* **75** (2007) 083511; S. Pascoli, S. T. Petcov and A. Riotto, *Nucl. Phys. B* **774** (2007) 1; K. Moffat *et al.*, *Phys. Rev. D* **98** (2018) 015036; K. Moffat, S. Pascoli, S. T. Petcov and J. Turner, *JHEP* **1903** (2019) 034.
- [165] R. K. Sachs and A. M. Wolfe, *Astrophys. J.* **147** (1967) 73 [*Gen. Rel. Grav.* **39** (2007) 1929].
- [166] D. J. Eisenstein and W. Hu, *Astrophys. J.* **511** (1997) 5.
- [167] M. Tegmark *et al.* [SDSS Collaboration], *Astrophys. J.* **606** (2004) 702.

- [168] F. Beutler *et al.* [BOSS Collaboration], *Mon. Not. Roy. Astron. Soc.* **444** (2014) 3501.
- [169] G. J. Hill *et al.*, *ASP Conf. Ser.* **399** (2008) 115.
- [170] T. Abbott *et al.* [DES Collaboration], astro-ph/0510346.
- [171] N. Palanque-Delabrouille *et al.*, *JCAP* **1511** (2015) 011.
- [172] S. Hannestad, H. Tu and Y. Y. Y. Wong, *JCAP* **0606** (2006) 025; M. Kaplinghat, L. Knox and Y. S. Song, *Phys. Rev. Lett.* **91** (2003) 241301; R. A. Battye and A. Moss, *Phys. Rev. Lett.* **112** (2014) 051303.
- [173] S. Dodelson and L.M. Widrow, *Phys. Rev. Lett.* **72** (1994) 17.
- [174] K. Abazajian, G. M. Fuller and M. Patel, *Phys. Rev. D* **64** (2001) 023501.
- [175] X.-D. Shi and G.M. Fuller, *Phys. Rev. Lett.* **82** (1999) 2832; K. Petraki and A. Kusenko, *Phys. Rev. D* **77** (2008) 065014; M. Shaposhnikov, *JHEP* **08** (2008) 008; M. Drewes *et al.*, *JCAP* **01** (2017) 025.
- [176] For a review see e.g. A. Mirizzi *et al.*, *Riv. Nuovo Cim.* **39** (2016) 1.
- [177] K. Scholberg, *Ann. Rev. Nucl. Part. Sci.* **62** (2012) 81.
- [178] V. Trimble, *Rev. Mod. Phys.* **60** (1988) 859.
- [179] K. S. Hirata *et al.*, *Phys. Rev. D* **38** (1988) 448.
- [180] C. B. Bratton *et al.*, *Phys. Rev. D* **37** (1988) 3361.